



The Department of Civil and Architectural Engineering

Degree project in Building Services and Energy

Second cycle, 30 credits

Analyses of particulate matter movement between neighboring windows

Computational fluid dynamics study

IBRAHIM AL-BWAB

PREFACE

This master thesis is directed towards the recent events occurring 4 years ago when SARS-CoV-2 pandemic was acknowledged worldwide. This pandemic refined our understanding of pathogens, their transmission medium, and the likelihood of causing an infection. To elaborate on this matter, airborne transmission of SARS-CoV-2 was recognized and confirmed to occur in closed spaces, and its possibility to be suspended in the air indefinitely. Thus, a risk of using practices in the building environmental sector such as natural ventilation might induce a problem where SARS-CoV-2 perhaps can travel over distances between neighboring windows of different accommodation units, thus, increasing the likelihood of individuals that happen not to be in the same room to infect each other based on the assumption that one of these individuals is sick and experiencing symptoms such as coughing which is identified as a common symptom of being infected with SARS-CoV-2. Coughing itself isn't the only main way to disperse the virus-laden, whereas it was identified that respiratory activities in the form of speaking, breathing, and talking can induce a risk as well. This matter was thus examined in reference to its likelihood of happening.

ABSTRACT

To assess the possibility of this matter, natural ventilation was explained in relation to why individuals would consider using this type of ventilation in enclosed places and what parameters it depends on. Upon understanding those parameters and weighing their importance, several cases were identified to be examined using computational fluid dynamics tools to see the probability of this virus-laden particle to undergo a traveled trajectory between neighboring windows through the four dimensions of space and time. Thus, the case would then confirm if such a matter, if possible, occurs over distances where both indoor and outdoor conditions are simulated. It was also acknowledged that if these viruses happen to undergo such a trajectory, it would be a matter of likelihood to cause another individual to be infected since environmental conditions play a significant role in the natural decay of these airborne viruses.

SUMMARY

To summarize the outcome of this thesis, transmission occurs in three forms: fomite, near contact, and airborne. Further, air can be shared between individuals across the building sector through elevator use and openings. Furthermore, thermal comfort is a leading aspect of why certain individuals would engage in practices such as natural ventilation. Through the use of such a practice, the airflow rate obtained at an opening depends on several conditions in terms of temperature differences, wind direction, and velocity. Thus, the outcome can be different based on such factors. The transmission of virus-laden couldn't be assisted in this thesis due to persisting problem with the tool used. Thus, it is important to have a deep understanding of fluid dynamics and ensure that steps taken comply with realistic physics properties to achieve an accurate solution. The problem persisting is explained in the discussion section of this master thesis, and mitigation is specified as well. It is, however, important to acknowledge that mitigating the problem was not achieved.

ACKNOWLEDGMENT

I would like to express my gratitude to Wei Liu, my supervisor through my master's thesis, which focuses on topics concerning sustainable energy and environmental engineering at KTH Royal Institute of Technology in Stockholm, Sweden. Throughout the master thesis, W. Liu provided me with the necessary guidelines and ensured that the trajectory of my track was correct to achieve the objective of the following study.

Throughout the master's thesis, however, issues persisted with the tool used to simulate fluid dynamics to achieve the objective and ensure the accuracy of my calculations necessary to obtain results. Thus, help was needed and requested from Giovanni Calozari, a researcher and academic staff member at KTH in the fields of system engineering, computer science, and industrial engineering.

I would like to extend my deepest gratitude to Ivo Martinac, the examiner of this master's thesis and a professor at KTH, for assisting me with the necessary help to come to a conclusion of this master's thesis. The objective failed due to unfamiliarity with the tool used, which then caused a persisting issue that disallowed me to obtain results. Guidelines and an initial process were however followed to make sure that no problems would occur.

TABLE OF CONTENT

1. Introduction	6
2. Literature review	7
2.1 Transmission routes.....	7
2.2 Transmission in Buildings.....	12
2.2.1 IEQ (Indoor environmental quality).....	16
2.2.1.1 IAQ (Indoor air quality)	16
2.2.1.2 Thermal comfort.....	17
2.2.1.3 Visual comfort.....	18
2.2.1.4 Acoustic comfort	19
2.2.2 The need of natural ventilation.....	20
3. Methodology	22
3.1 Induced danger of opening windows and study choice.....	25
3.2 Building envelope opening flows.....	27
3.2.1 Buoyancy effect.....	27
3.2.2 Wind effect.....	28
3.2.3 The combined effect of buoyancy and wind velocity	29
3.2.4 The combined effects of buoyancy, wind velocity and direction	30
3.3 CFD	31
3.3.1 Overview of ICEM.....	36
3.3.1.1 Geometry setup	37
3.3.1.2 Grid setup	40
3.3.1.3 Grid elements count and quality.....	41
3.3.2 Overview of Ansys Fluent and turbulence engineering	43
3.3.2.1 Wind.....	46
3.3.2.1.1 Windrose analysis	47
3.3.2.1.2 Wind turbuelnce engineering	50
3.3.2.2 Turbulence modeling and governing equations	53
3.3.2.3 Boundary conditions	56
3.3.2.3.1 Natural convection	56
3.3.2.3.2 Energy setup.....	58
3.3.2.3.3 Cough dispersion.....	59
3.3.3 Results	61
4. Discussion	66

5. Conclusion.....	70
6. References	71
A. Appendices	75
A.1 Appendix	75
Wells Riley equation	75
A.2 Appendix	75
Predicted mean vote equation	75
Predicted mean vote equation	76
A.3 Appendix	76
A.4 Appendix	76

1. Introduction

Viruses are classified as pathogens that can replicate by infecting a cell body, which then becomes a host cell for the virus. These pathogens are small genetic information that is plain in structure and composed of DNA or RNA and a genomic material enclosed by a proteinaceous capsid. If they find a host, they tend to encode their genetic sequence into the host cell and reproduce. This process is necessary because viruses do indeed lack the structure needed to be a cell, and thus, a cell is needed for them to be able to replicate. Their structure and composition should be understood to separate and classify these pathogens. Since the beginning of the 13th century, Stanley, Bernal, and Fankuchen have examined these pathogens, seeking to understand their structure by studying the tobacco mosaic virus “TMV.” They then separated these pathogens into two types: Enveloped and non-enveloped viruses. Primarily, the names were acclaimed by the presence or absence of lipid bilayer membranes on their shell body. In general, non-enveloped viruses are considered more pernicious than enveloped viruses due to their structure, which increases their survival rate in harsh environmental conditions such as extreme PH, temperature, and range of humidity values. [101] [102]

The research objective of this thesis focuses on evaluating the transmission routes in the building sector and understanding how environmental conditions such as temperature difference, air velocity, and direction can impact the transmission of these pathogens. The objective is to further assess the cases necessary to obtain results on how these pathogens can transmit between neighboring open windows.

The structure of this thesis thus follows to explain the transmission routes of pathogens, their effect on buildings in terms of places that accommodate risk, and the reason behind engaging in practices that these places with accommodating risk would be used. Further two research questions were evaluated to be important in assessing such a transmission and to identify the cases necessary to be examined

2. Literature review

2.1 Transmission routes

However, enveloped viruses are less pernicious than non-enveloped viruses due to their enveloped structure and non-causation of cell lysis when they exit the host cell. In the following thesis, Enveloped viruses are of particular interest due to the recent events of “COVID-19,” which the World Health Organization classified as a pandemic at the beginning of the 22nd century. The classification of SARS-CoV-2, along with many other viruses such as influenza, Herpesviridae family “HSV-1” and “HSV-2”, Human Immunodeficiency Virus (HIV), and Respiratory Syncytial Virus “RSV”, falls under the lipid-virus category. This category classification doesn’t, however, provide absolute classification criteria on their preferred medium of transmission as each, in fact, has a preferred medium of spreading due to its ability to infect different types of cells. By looking at the Human Immunodeficiency Virus, it is considered to be a retrovirus primarily infecting the immune system, especially CD4-positive T-cells. On the other hand, SARS-CoV-2 doesn’t infect the same cells and primarily infects the respiratory tract system. [101] [102]

Perhaps a better way to classify these viruses would be by their capabilities and preferred transmission medium, which can be direct, indirect, or airborne.

Concerning humans, Direct transmission occurs through direct contact with an infected person through different social activities that require a physical touch, such as the formerly mentioned viruses Herpesviridae family viruses and the Human Immunodeficiency Virus “HIV”. Whereas fomite and airborne transmission occur through water vapor molecules expelled through different expiratory activities such as breathing, coughing, sneezing, talking, and singing. In differentiation of the mentioned transmission routes, these expelled vapor molecules are size-dependent as droplets measuring less than 5 μm in diameter are referred to as airborne droplet particles, and droplets bigger than 5 μm understood as indirect (fomite) transmission mainly because these droplets drop to surfaces which become contaminated due to gravity settlement within (1-2m) distance from the host location. This occurrence happens due to the size of those expelled droplets as their mass increases as a function of their size. Whereas airborne droplets, also referred to as aerosols, tend to rise after being exhaled or

dispersed through expiratory activities due to temperature differences between the host and the surrounding environment and surrounding air direction. Their trajectory and settlement time are then influenced by the body’s thermal plume, ultraviolet radiation “UV”, airflow, relative humidity, and temperature. [103]

In the context of the SARS-CoV-2 pandemic, the World Health Organization (WHO) considered in February 2020 that the transmission of SARS-CoV-2 was considered to occur through indirect contact (fomite). Derived from the information received by the organization, countries acted upon the following statement by regulating a 2-meter distance between individuals as a mitigation to stop the super-spreading observed worldwide. Following the statement, the agency unambiguously stated the virus is still considered to be not airborne even though numerous studies embarked on addressing the possibility of airborne transmission. Gradually, WHO acknowledged the possibility of airborne transmission of the virus. Although airborne transmission was acknowledged, the initial time to address that possibility took 2 years. [104] [105] [106] [107] [108] [109] [110] Throughout the consideration of Airborne transmission, it was found that 80-90% of the droplets generated by respiratory activities fall indeed below 5 µm which can be accumulated in badly ventilated areas and survive for an extended amount of time and perhaps infect individuals who might happen to exist at that space and time of these aerosols to cause an infection. [110]

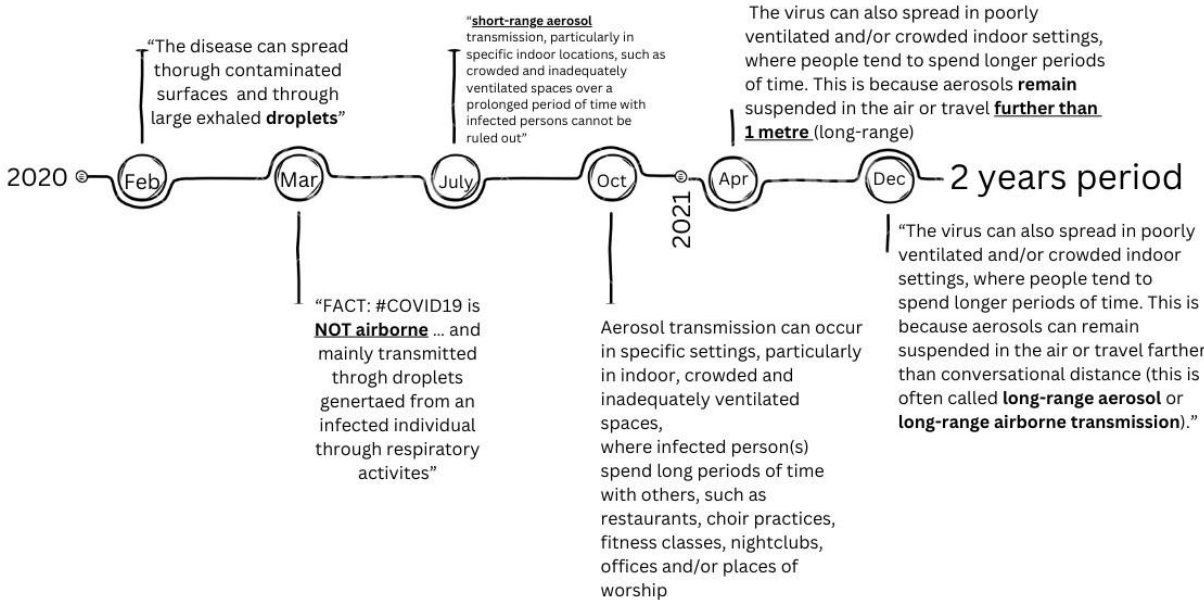


Figure 1: WHO timeframe of evaluating SARS-CoV-2

To assist the risk of infection, one must understand the absolute value of the residual time of these pathogens once they are dispersed through different respiratory activities. One study, like many others, assisted the residual time of a scatter of different diameters of aerosols once they are expelled into the surrounding environment of the infected individual. For aerosols with a diameter of 10 μm , it took 17 minutes before settling. Whereas, 20 μm and 100 μm took 4 minutes and 10 seconds, respectively. However, aerosols with a diameter of 1-3 μm remained suspended almost indefinitely throughout the time measured. [109] [111] [112]

Understanding these pathogens through their viability is crucial. It's implied that once they leave the host through respiratory activities, they undergo natural decay and become deactivated over time under the influence of different environmental factors. Such environmental factors were mentioned earlier and give an insight into the decay of these pathogens. Different engineering methods are used to validate and assist in the natural decay of viruses. Such methods involve air and surface wipe sampling to further assess these viruses' viability. For the time being, Real-time Reverse Transcription Polymerase Chain Reaction "RT-PCR", Electron Microscopy "EM", and Immunofluorescence Assay "IFA" are commonly used as methods of identification. Each method has its own strengths and limitations, but each grants high precision in assessing the decay of these viruses. As this study addresses airborne transmission, once air samples are collected, viability is then identified through injection of such samples in one of these two widely used cells, Vero E6 cells and LLC-MK2 Cells, and then facilitate the replication occurring in the cells. [113] [114] [115] [116] In terms of understanding the values and conditions associated with either enhancing or diminishing the median half-life of lipid viruses in different conditions, a study was directed towards the role of ambient temperature and humidity in inactivation rates of enveloped viruses. The findings of the study determined that the higher the temperature, the more rapid the decay experienced by the enveloped virus in the study seen in figure (2).

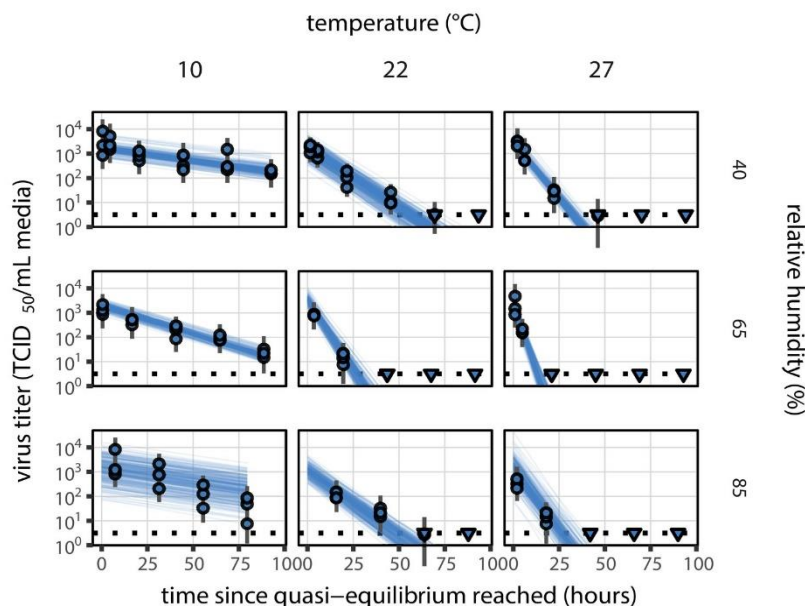


Figure 2: inactivation of virus-laden due to temperature and relative humidity

While it was observed, the inactivation of the enveloped virus decreased at extreme relative humidity levels, creating a V-shaped function seen in Figure (3). Furthermore, an increase in ultraviolet radiation index did indeed increase the deactivation rate in enveloped viruses. [114] [115] [116] [117]

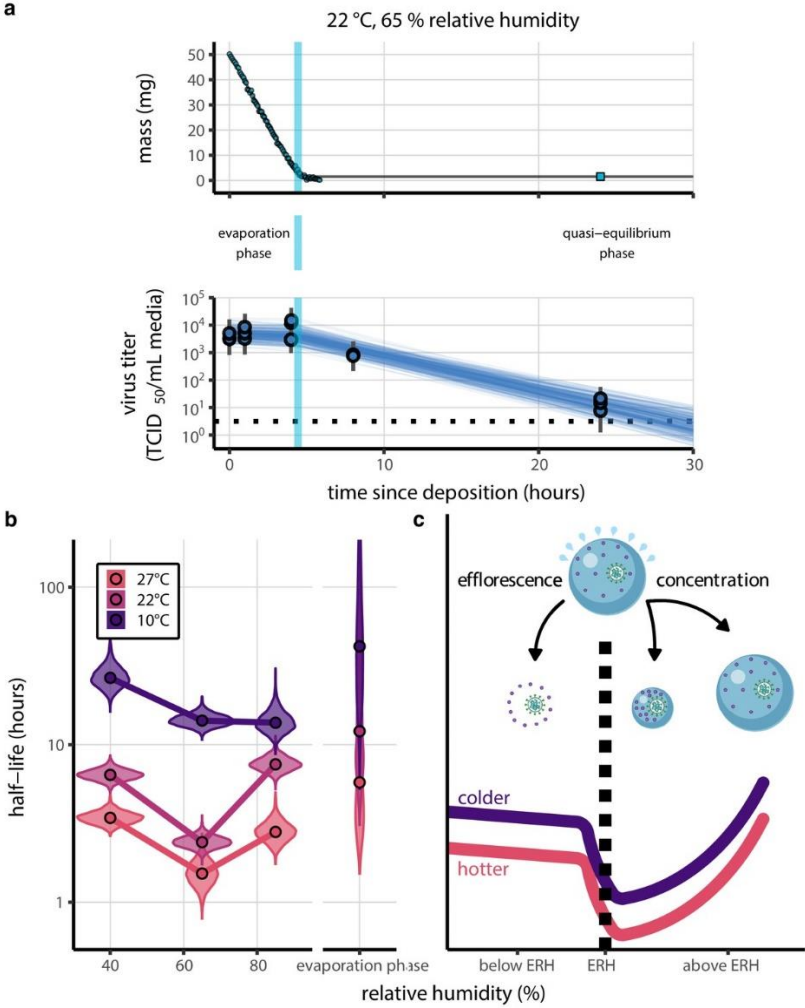


Figure 3: (a) Loss of mass due to evaporation and concentration of virus titer as function of time
 (b) Half life of Virus-laden due to temperature
 (c) deactivation of virus-laden due to relative humidity

2.2 Transmission in Buildings

In developed regions, People spend 87-90% of their time in indoor places. These include homes, schools, workplaces, worship houses, and restaurants. Under crowded scenarios, an imposed risk of the elevation of contaminants is questioned. Such contaminants include biological contaminants, Radon, Carbon dioxide, Nitrogen dioxide, industrial and office products, and many others. [118] To be in a position to mitigate such problems, adequate ventilation systems, such as mechanical systems, are required to decrease the amount of contaminations indoors. The American Society of Heating, Refrigerating, and Air-conditioning Engineers “ASHRAE” and The Federation of European Heating, Ventilation and Air-Conditioning Associations “REHVA” Provides guidelines through standard practices on how Heating, Ventilation, and Air-Conditioning should be designed to ensure good¹ Indoor Air Quality (IAQ). [119][120][122] According to the compliances provided by ASHRAE, such measurement of good air quality refers to the lack of contaminants where the dissatisfaction of occupants doesn't exceed 20%. [129]

During the COVID-19 pandemic, ASHRAE and REHVA provided better guidelines to limit the spread of infection based on the existing evidence on airborne transmission possibilities. [121]

The World Health Organization also provided measurements in indoor scenarios to evade the risk of infection during the COVID-19 pandemic. These measurements explicitly addressed the population to avoid gatherings as a form of social distancing and maintain acceptable hygiene by frequently washing hands and using hand sanitizers. [123] Another proposed measure was the use of face masks in public. [123] These earlier proposed measurements mainly addressed a reduction of the infection risk. [124] Although following these practices did minimize short-range transmission, it didn't stop the super-spreading of the SARS-CoV-2. This can be explained by the lack of airborne measurements and acknowledging the possibility of long-range transmission early in the pandemic. Face masks do indeed help with short-range transmission due to their ability to filter droplet particles, but they lack the ability to filter small-diameter droplet nuclei. Face masks of type N95 are capable of such filtration but weren't necessarily addressed by the World Health Organization to be used by the public. [123] [124]

¹ Meeting the standards of indoor air quality set by ASHRAE and REHVA through studies and measurements.

Following such events, many studies addressed the possibility of long-range transmission. On the 10th of March 2020, a super-spreading event occurred in indoor settings in The Skagit Valley Chorale. This notable incident happened in the early stages of the pandemic and gained attention to the possibility of airborne transmission. 50% attendance of the total members showed up to the event, where some measurements were taken. Such measurements include 1.4 meters distance in the same direction and 0.75 meters in the perpendicular direction between neighboring chair centres. Further into these measurements, limited social activities among the members were regulated, hand sanitizing was available, and sanitation services were used by 8 out of 61 chorale members. During the event, air temperature was measured at 20°C and relative humidity at 53%. The event outcome showed an infection rate between 53 and 87%, where 53 out of 61 members tested positive within a 2-week period. With such measurements, Fomite and short-range transmission can't explain the observation made of the outcome. [125]

Another super-spreading event occurred as early as January 2020 in a poorly ventilated restaurant in Guangzhou, China. At that time instance of the event, only 322 cases were reported positive worldwide, and one individual had positive symptoms of having SARS-CoV-2 at the restaurant. The event consisted of 3 families of 21 members in total sitting at neighboring tables. These 3 families were reported not having a social encounter with inhabitants from Hubei, where the outbreak started. Within 2-week period, 9 members of these 3 families tested positive for SARS-CoV-2. Further assessment using Computational Fluid Dynamics "CFD" with the same settings was made to identify the possible residence time of air in the restaurant. The ventilation rate was measured at 0.9 L/s.person which didn't meet the requirement standard of ASHRAE 62.1-2019 of 8-10 l/s.person. [126] However, at the same time, ASHRAE 62.1-2019 standard doesn't accurately reflect the minimum required ventilation rate needed to limit the possibility of airborne transmission. A better approach is to use the Wells-Riley equation, a mathematical model that can be used to assess the risk of airborne transmission of respiratory infectious diseases ^{Appendix A.1}. The equation can be used to identify the minimum required ventilation flow rate needed if the quanta generation of the virus is known. Despite the following, the quanta generation of SARS-CoV-2 isn't fully known at the time being, and further assessment can't be accurately presented. [126] [127] [128]

Further into assessing the possibility of airborne transmission in indoor places, a systematic literature review was carried out in the second year of the pandemic to address the possibility

of the presence of infectious viruses in air in enclosed places. The locations chosen were residual buildings, hospitals; empty and occupied, clinics, isolation rooms, and laboratories. Using the different techniques mentioned earlier, such as RT-PCR, EM, and IFA, the viability of RNAs in Droplet nuclei were measured. 11 cases were analyzed that were built upon the locations mentioned, and Severe Acute Respiratory Syndrome family viruses: SARS-CoV-1, SARS-CoV-2, and MERS-CoV were addressed. Proceeding into findings, Virus presence was confirmed in 10 cases, where the RNA was still viable in 7 cases. [105] Another case in buildings where air is shared is in the elevator. Although the residence time in the elevator is usually less than a minute, 3 cases were built upon breathing and talking; with ventilation and without. The risk of infection was facilitated by using the Wells-Riley model; the findings showed that using ventilation reduces the airborne nuclei particles in shared air, thus lowering the risk of infection. [130]

So far, the contamination source is assumed to exist indoors and therefore, concentration of such droplet nuclei increases over time if no adequate ventilation system exists in such indoor settings. How about out contamination of Severe Acute Respiratory Syndrome family viruses in outdoor air?

A systematic review was carried out in outdoor places within close-proximity to healthcare units, parks, and industrial places. RNAs were detected close to healthcare units and industrial places but not in open areas such as parks. As for such studies, the place of air sample measurements is unidentified, and no further viability tests were taken as well. Thus, no correlation between close-proximity and air sampling can't be taken definitely due to the lack of detailed settings and viability measurements. [131] However, throughout the systematic review, a conclusion on the possibility of pollutant transmission between indoors and outdoors is highly likely throughout openings and ventilation systems. Still, the previous statement highly depends on the definition of space and time, as urban air quality isn't absolute in every space and time. To understand the definition of space in this context, each region differs from another in urban air quality due to different regulations set by the region. [132] [133] However, time is a different aspect, and certain times can verily influence urban air quality. Due to observations made by different studies in divergent places, a sudden drop in different contaminations occurred when human activities were heavily restricted during the first year of the COVID-19 outbreak. [134] [135] [136] [137] [138] Parallel in context, a low carbon emission trend was observed due to the restriction of outdoor activities. Such activities include the use of motor vehicles and machinery in factories. [134]

Throughout the previous paragraph, it's understood that air pollutants can be transmitted between indoors and outdoors. It is fair to mention that three major factors affecting the possibility and the transmission rate are considered to be mechanical ventilation, infiltration, and natural ventilation. [139] [140] However, other factors such as local weather conditions, temperature differences between indoors and outdoors, topography, and the human thermal plume can change the outcome of transmission. [139] [140] In mechanical ventilation practices, air filtration properties and ventilation ducts used in mechanical ventilation systems lead to different outcomes regarding particulate matter transmission between indoor and outdoor environments. [141] [142] [143] [144] [145] Infiltration was another side that determines particulate matter transmission between indoors and outdoors. To elaborate, Infiltration is understood as unintentional particulate matter transmission between indoors and outdoors due to various openings, cracks, and gaps in the building envelope that happen to exist or develop under faulty practices and mistakes in fabricating a building during the construction phase. These flaws can also be time-related due to the degradation of materials during the operational phase. Aspects such as construction quality, air pressure differences, cracks formation and structure, and size of particulate matter in question can influence the outcome of transmission. [144] [145] [146] Natural ventilation is another viewpoint that affects the transmission rate. Occupants present in indoor settings often engage in opening and closing windows and doors, consciously and unconsciously, caused by experiencing discomfort and seeking a change in the Indoor Environmental Quality "IEQ" state. [134][147]

2.2.1 IEQ (Indoor environmental quality)

To grasp the idea of IEQ, Indoor environmental quality “IEQ” is a broad aspect that relates to the state of health, comfort, and productivity of occupants in indoor settings. [149] To elaborate on the previous statement, Indoor environmental quality can be explained by its sub-categories. These sub-categories are Indoor Air Quality (IAQ), thermal, acoustic, and visual comfort. [149]

2.2.1.1 IAQ (*Indoor air quality*)

Starting with indoor air quality, “IAQ” is defined as the state of air that is considered free of harmful contaminants and odours at concentrations that are deemed safe by authorities such as ASHRAE and REHVA, and at which dissatisfaction is at the most experienced by 20% of the exposed population in the indoor settings. [148] such contaminants are mentioned earlier and can lead to dissatisfaction or reduced productivity. In a sense, when the following state is experienced by the exposed population, Natural ventilation is used to filtrate out such contaminants and reduce their concentration in indoor settings. During the COVID-19 pandemic, The Chinese Health Commission suggested opening windows for at least 30 minutes multiple times a day in a room where an infected person is self-isolated to drive away contamination’s concentration in the room. Upon the following recommendation, [150] examined the effectiveness of this method in 6 different settings with 3 different room geometries. The following study didn’t address airborne particle concentration due to the lack of measurement on SARS-CoV-2 quanta generation but rather examined the exhaled Co₂ concentration indoors as a measurement of indoor air quality criteria with a function of air exchange rate through the opened window. The results showed that CO₂ levels reached equilibrium with the outdoor environment $CO_2 = 400 \text{ ppm}$ when the air change rate “ACH” was measured at 5 cycles per hour with no further improvement at a higher air change rate. [150] This study highlights the importance of natural ventilation in improving air quality and as well amplifying the recommendations made by the Chinese health commission.

2.2.1.2 Thermal comfort

Thermal comfort is another sub-category of IEQ, and it refers to the state of mind that conveys satisfaction with the surrounding thermal environment. [154] In the context of building services, this state of mind can be achieved when occupants in indoor settings feel neither too hot nor too cold; instead, they sense and express satisfaction with the surrounding thermal environment. [154]

Certain factors, such as environmental and personal, must fall within a range to achieve the mentioned state. ISO 7730 standardized a method to give an insight into these conditions and methods of predicting discomfort levels associated with these environmental and personal factors through Predicted Mean Vote “PMV” and Predicted Percentage Dissatisfaction “PPD” indices. [154] [155] [157] [158] Starting with the factors mentioned, the key environmental factors are 4 and include air temperature, radiant temperature, air velocity, and humidity. The personal factors are two: clothing insulation and metabolic rate.

As for defining each factor and understanding its importance of them, air temperature is the first environmental factor and refers to the actual temperature of air measured in an indoor environment, commonly measured in Celsius “C” or Fahrenheit “F”, which depends on the standard temperature measurement unit used in different regions. However, radiant temperature specifies the heat that is radiated from surfaces such as electronic devices, occupants, and building components, e.g., walls, windows, and floors. Unlike air temperature, the radiant temperature is considered a local, near-proximity property. Thus, different occupants in the same room might express thermal satisfaction in different senses due to distance from radiative heat objects. The third factor is air velocity, which stands for the local air velocity moving by an occupant. air velocity might enhance heat loss dispensed by an occupant as a result of enhanced heat convection and evaporation. The last environmental factor is humidity, which has an influence on the rate at which the skin can sweat, and therefore, humidity changes the perception at which the thermal condition can be perceived. [156] [154]

Commencing on the personal factors, Clothing insulation is the first aspect, and it is understood as the provided thermal insulation between the occupant and the surrounding environment on account of clothes heat insulation. Clothing insulation is typically measured by clo units, which is a measurement that is specified by ASHRAE standard 55, ISO 7730,

and EN 15251. [156] [154] Further, regarding personal factors, metabolic rate measures the pace at which the occupant produces heat through metabolic processes to maintain a stable internal temperature, which is crucial for the occupant's comfort. [156] [154] As mentioned, metabolic rate is a personal aspect. It differs between individuals, which influences the absolute satisfaction rate of all occupants and deviates from the resulting dissatisfaction in the same indoor settings in terms of heat, ventilation, and air conditioning. Activities change the metabolic rate measured in MET units, e.g., 1.0 for a seated, relaxed occupant and 1.2 for sedentary activities such as typing, seated in an office. [159] Another way of measurement is by watts per square meter [W/m^2]. e.g. 58 [W/m^2] and 70 [W/m^2], respectively, for the same activities mentioned above in MET units. Square meters as of human skin surface e.g. 1.8 m^2 of an average human. [159] ASHRAE 55 standard provides measurements of different activities in these units to further assist thermal comfort indoors experienced by an occupant or an individual. [159] Likewise, illness or infection, e.g., respiratory illness, increases the body temperature in cases like SARS-CoV-2, causing fever, which then influences the body's metabolic rate and increases it [151]. [152] found that by measuring 6 different infections that cause fever, the metabolic rate on average increases by 13% for each one-degree Celsius increase in body temperature above baseline². In such a sense, infection increases thermal dissatisfaction experienced by a sick individual. Thus, an infected individual engages then in adaptive behaviors such as using natural ventilation to lower the thermal dissatisfaction experienced.

2.2.1.3 Visual comfort

Visual comfort, however, concerns the quality of visual satisfaction in a building environment [160]. To ensure that occupants experience visual satisfaction, the lighting environment should be adequate for the activities being performed without causing glare or having insufficient illumination. Light can be controlled through artificial lighting and natural lighting. [160] At first, natural light should be emphasized and then complemented with artificial lighting if necessary, owing to the fact that natural light is more comfortable for human eyesight, whereas natural light is a source of illumination that the human's eyesight adapts to conveniently. [160] However, natural light availability and intensity can be a

² Average human body temperature 36.5-37.5 C

challenging aspect. Hence, as mentioned, artificial light can be used to complement the natural light source by appropriately considering the placement and the light distribution needed for the activity in question. [160]

2.2.1.4 Acoustic comfort

The last aspect of IEQ is acoustic comfort, which addresses the auditory environment in a building where an occupant experiences satisfaction with the surrounding acoustic conditions. [162] To control this aspect, noise should be regulated in the indoor environment with techniques such as adequate insulation materials and sufficient window thickness with multiple glazing. [163] These methods are commonly used to control the noise promoted from the building's surrounding. However, noise can be categorized into white, pink, brown, blue, violent, grey and background noise. Each has different behaviors in frequency and sound patterns. Concerning building environment, white and background noise are widely common where, white noise refers to the type of noise that contains equal power across all frequencies within the audible spectrum, meaning it is characterized to be uniform and continuous. [162] On the other hand, Background noise is tied to the classification of being varied, meaning it can be sudden and dynamic in frequency, e.g. people speaking in close-proximity, doorbells, and traffic noise. In relation to occupant comfort, [164] found that background noise of magnitude 40 dB(A) and white noise of 85 dB(A) did not alter the occupant's acoustic comfort. The previous statement highlights the differences of magnitude associated with uniform and dynamic noise spectrums on occupant comfort. To summarize, acoustic comfort is achieved by preventing the development of audible inconvenience.

2.2.2 The need of natural ventilation

As mentioned earlier, occupants open windows and doors, consciously and unconsciously, to Improve the “IEQ” state of an indoor environment. As understood from defining and analyzing the sub-categories of “IEQ”, opening windows and doors is a common practice to improve the IEQ state experienced by an occupant. What that signifies is a change in either one of the sub-categories of IEQ or multiple of them by an occupant is sought. Conceivably, a better understanding of weighing IEQ sub-categories is needed in terms of their effects and preferences on occupants indoors to understand which of these sub-categories would probably be a leading cause to open a window. [165] Examined how IEQ sub-categories are weighted by in terms of prioritization and importance by reviewing the following studies [166] [167] [168] [169] [170] [171] [172]. These studies are performed by filling out questionnaires performed by building users such as visitors and occupants with no control over the absolute distance to openings such as windows and doors. These questionnaires were administered in offices, homes, and schools. These studies' findings showed a higher weight to thermal and indoor air quality comfort and a slight reduction in importance to acoustic and visual comfort. However, these sub-categories were weighted differently with respect to sex, occupation time as of visitor or occupant, and the absolute distance to windows. Moreover, the place of study in terms of the country changed the ranking outcome, which highlights the importance of outdoor air quality in terms of satisfaction experienced. It is necessary as well to keep in mind, the outdoor conditions in terms of acoustics wasn't specified in these studies.

Fortunately, [165] examined two other studies as well [173] and [174]. Both of the following studies were conducted in a climate chamber, which is defined as a controlled environment used to test certain effects in question with systematic control over other environmental factors. The results in both studies showed the same magnitude of importance for thermal comfort. A 1 degree of change in celsius of the operative temperature corresponded to the same discomfort experienced by the occupants in question in order of change in acoustic by 3.8 db(A) and 3.9 db(A). Nevertheless, the type of noise wasn't specified in these studies.

Understanding the importance of thermal comfort on occupant behavior and engaging in practices such as the use of natural ventilation to improve thermal comfort is crucial. It is necessary to define a way to predict the discomfort experienced by the same occupant in certain indoor settings. One way, as mentioned earlier, is the use of Fanger's comfort equation, which was established in the 1970s and complies with ISO 7730. [176] Fanger

equation ^{Appendix A.2}, can be used to predict thermal comfort in indoor environments. The equation was developed by the Danish engineer P.O. Fanger and considered a core element to calculate the Predicted Mean Vote “PMV” and Predicted Percentage Dissatisfied. PMV is a quantitative index that measures thermal sensation in indoor settings based on the factors mentioned earlier: air temperature, radiant temperature, air velocity, humidity, clothing insulation, and metabolic rate. [176] This quantitative index has a seven-point scale ranging between -3(sensing cold) to 3(sensing hot). Once solved, PPD can be then calculated, and ranges between 5-100% dissatisfaction. The motive behind a minimum value of 5% dissatisfaction is human variability in being thermally dissatisfied. To elaborate, factors such as clothing insulation and metabolic rate can differ from one person to another, meaning a thermal environment can be quite challenging to design to account for such factors when the same air is shared in indoor settings. [175]

Additionally, The Organisation for Economic Cooperation and Development (OCED), in its work on reducing CO₂ emissions and improving indoor air quality, has estimated that the residential and commercial building sectors account for 30-40% of all primary energy and natural resource use during a building's life span. It is understood that 80% of this energy use takes place in the building's operational phase. Half of this energy used in the operational phase of a building is consumed by HVAC systems and thermal comfort. [177] [178] The use of natural ventilation is then preferable in terms of cutting down energy use consumed on HVAC systems [179]

3. Methodology

As understood from reviewing the literature on lipid-enveloped pathogens, Indoor environmental quality, and natural ventilation, it implies that natural ventilation is a method used in the building environment sector to control the airflow rate in a place or a room, which was mentioned earlier. To elaborate, natural ventilation can be explained as the procedure of fresh outdoor air seeking its way to a place or a room but in a way that occurs naturally. With naturally, it is meant that the air seeks its way without the use of mechanical support such as the use of forced convection methods, e.g., operational fans. In the context of natural ventilation, external airflow properties in the sense of indoor and outdoor air pressure differences and air direction influence the air flow rate at an opening. It's necessary to acknowledge that natural ventilation isn't a new method that is used in the building environment to ventilate indoor places and has been used over a wide time scale. Its popularity mainly relies on the fact that natural ventilation provides fresh air with low carbon dioxide emissions, as mentioned earlier while it induces a reduced energy consumption due to the limited use of mechanical ventilation. There are three methods of natural ventilation these methods are, single-sided ventilation, cross-ventilation, and stack ventilation. Since some pathogens are considered airborne transmitted such as SARS-COV-2, the natural ventilation use in residential buildings can be at risk of being a way for viruses to spread among residential units, giving some unit/s is/are contaminated with the virus through sick occupant/s residual time in this/these unit/s. Thus, quantifying the amount of contamination is an aspect that depends on numerous factors since those factors can change the range and the direction of the distance that the virus can travel. These factors can be environmental and operational. Environmental factors are outdoor and indoor temperature differences, wind velocity and direction. Operational factors are indoor airflow caused by a combination of natural and mechanical ventilation, geometries of the units, type of natural ventilation, and the size of the opening through which natural ventilation is set to occur. By the combination of natural and mechanical ventilation, it's meant that the air exchange rate that occurs through mechanical ventilation influence the airflow pattern of indoor air while using natural ventilation. Further into the following, if natural ventilation is set to occur through an opened window, mechanical ventilation is still operating, and thus, the dispersion of air is influenced by mechanical ventilation.

In the following thesis, an assumption of inoperable mechanical ventilation is considered, and only the effects of natural ventilation on the transmission of particulate matter through opened windows, which happen to be opened in parallel with time. To understand, the events of opened windows and virus dispersion are assumed to occur simultaneously. A well-mixed air condition indoors and outdoors is also assumed. The results of such an assumption then imply homogenous conditions for temperature, humidity, and other pollutant concentrations in space which simplifies the situation where wind magnitude and direction would be the leading route for particulate matter transmission.

However, since airflow rate can be influenced by temperature differences, and wind magnitude and direction, the first research question is, how is the airflow rate obtained at the opened window influenced due to temperature differences, wind magnitude and direction, and a combined effect of both of these factors?

The question can be answered by researching topics such as wind tunnel experiments on air flow rate change due to different air magnitudes and directions and providing numerical models to assist the airflow rate magnitude. The results would also give insight into the importance of studying the next question by altering the direction and magnitude since, in the second question, the well-mixed air condition is assumed.

The second research question is then set to be, how many aerosols can one contaminated unit transmit to another uncontaminated unit through the use of single-sided natural ventilation? The research question will help us understand the amount of pathogens transferred from one unit to another in single-sided natural ventilation use.

To answer the second research question, simulation made by a 3D Computational Fluid Dynamic model was chosen as a method. With the CFD models, wind magnitude and direction should be set. Rooms location, size, and relation of distance to each other shall be chosen. From researching similar topics, it's understood that there are a lot of parameters that should be taken into account. Such parameters are wind inlet magnitude and direction, as mentioned, and the importance can be known by answering the first research question. Further into identifying the parameters, area where natural ventilation is set to occur, the velocity of a cough, distribution, and frequency. Moreover, thermal plume effects on the dispersion should be understood since the sick occupant would be experiencing thermal discomfort and want to engage in opening the window to change the thermal state felt indoors. Further Heat flux conditions of indoor and outdoor walls shall be defined. Moreover, an appropriate wind

magnitude profile shall be researched and be chosen. A choice of suitable turbulence model for the study shall be appointed, Grid setup and boundary conditions shall be set.

3.1 Induced danger of opening windows and study choice

Due to the literature review made previously on natural ventilation's importance in the building environment sector, it is understood that natural ventilation is a promising aspect in improving indoor air quality and the thermal comfort of occupants if the conditions outdoors are within a range that induce a change to the occupant's thermal satisfactory. It also offers a beneficial reduction in energy use. However, In the recent pandemic of COVID-19, superspreading events weren't fully understood since lockdowns occurred in most of the countries, yet SARS-CoV-2 continued spreading. Through research, it is also understood that airborne spread can be the reason behind the superspreading and lipid viruses nuclei can be viable and present in aerosols for a set of time where airborne transmission can occur. Interestingly, the following thesis is directed towards the possibility of danger in the use of natural ventilation as a practice to improve indoor air quality, occupant's thermal state or to reduce the magnitude of energy use.

As of the study choice, such a study case is understood to be done in two manners. The first manner is that the study case can be a natural experiment, where the experiment takes place in a real-life situation. Now, of course, the experiment might work, but there might be some variables that can't be controlled as well. Thus, the experiment's numerical results can be falsely when considered at a wider scale than the experiment space and time choices. These unidentified variables can cause an issue where internal validity is not an issue, but external validity is. As mentioned, not all control variables can be controlled, and thus, the results obtained can't be generalized. To conclude, a natural experiment lacks the ability to allow for manipulation and control of all variables, thus making external validity uncertain. External validity is nevertheless less of a problem for a model. In a model, manipulation and controlling variables are possible. One can intervene with the variables in a model to see if a variable can cause a shift in the results of one's study. In a sense, Control of background variables can be achieved by using a simulation model. Using a simulation model is the second method, and it is considered time-effective and rather cheap to construct. Variables can be considered based on idealized or wishful situation/situations as well. Justification on the choice of variables will be provided later in the study upon guidelines recommended by similar studies. Another benefit is the simplicity of representations that a model can offer. One can simulate important aspects, making it easy to understand how certain variables influence the results. For instance, wind magnitude and direction that are used in this case

study. As models offer great advantages over experiments for the purpose of this case study, there are some disadvantages too. Such disadvantages can be the assumptions made to simplify the model in order to reduce the computational cost. This might lead to incorrect results if such variables are important in such a case study where a total reflection of the results in real life can't be explained with the simulation model due to the complexity of such cases in real life. Research later will increase confidence that those unknown variables can be neglected and still achieve accurate results. Another disadvantage is the accuracy of the outcome generated from the CFD application used to simulate the model based on the grid setup, surroundings of the chosen building, and the choice of turbulence model. In this case the application preferred is Ansys fluent due to earlier experience with the application. It's acknowledged that earlier experiences are not a valid reason for justification of application use, therefore, more research on the accuracy of the out data generated from the application as well as user satisfaction shall be done. One additional manner that can be possible to conduct such a study is a laboratory experiment where variables can be controlled since the study is done in an isolated lab. But this manner was excluded as an option since running this experiment requires finance, size and a lot of time. There is the unethical part of conducting an experiment as well where real life infection transmission should occur in such settings.

3.2 Building envelope opening flows

Up to now, this thesis has explained the importance and the need for natural ventilation. In natural ventilation, it is crucial to accurately predict airflow through windows for maintaining a healthy indoor environment and minimizing energy consumption. Unlike cross-ventilation, where the airflow rate is relatively well defined, single-sided ventilation poses challenges due to its unpredictable and often unsteady airflow patterns. Factors such as wind magnitude, direction, temperature differences, and turbulence characteristics influence the airflow rate obtained at single-sided openings. Empirical expression derived from wind tunnel improve and broaden our understanding of such a phenomenon in terms of the parameters mentioned earlier. However, predicting airflow in single-sided ventilation remains a complex matter due to the variability of these factors. Thus, the empirical expressions derived from wind tunnel experiments are indeed favourable. A description of equations parameters can be obtained at table (1).

Q_v	the volume flow rate [$\frac{m^3}{s}$]
C_D	The discharge coefficient
U_L	Local speed obtained at window [$\frac{m}{s}$]
U_R	Reference wind speed [$\frac{m}{s}$]
A_{eff}	effective area [m^2]
h	Height of window [m]
ΔT	Temperature differences [K]
$f(\beta)$	Function depending on incidence angle β
C_p	Pressure coefficient
A	Area of window [m^2]

Table 1: Description of parameters

3.2.1 Buoyancy effect

The buoyancy effect addresses airflow driven only by thermal effects on a single side ventilation where indoor air is heated due to occupants, appliances or sunlight heating the building materials. The air indoor then would tend to raise in temperature and flow upwards where a temperature profile would occur indoor relative to the height of the room. Once a single-sided window is open, the warm air escapes through the higher part of the opening, and cooler outdoor air enters through the lower part of the opening. In 1985, P.R Warren and L.M. Parkins in their paper named “Single-sided ventilation through open windows” explored the ventilation mechanism specific in single-sided ventilation. The paper presents a straightforward method predicting single-sided ventilation flow rate incorporated from theoretical models, wind tunnel experiments, and tracer gas measurements executed in real buildings. The paper discusses the findings and demonstrates how factors such as opening size, window type, and configurations affect the air flow rate. [224] P.R and L.M then derived the following expression to calculate the air flow rate.

$$Q_v = \frac{1}{3} \cdot C_D \cdot A \sqrt{\frac{(T_i - T_e) \cdot g \cdot (H_t - H_b)}{\bar{T}}} \quad (1)$$

3.2.2 Wind effect

For wind-driven ventilation obtained at a single-sided opening in a building envelope, the ventilation rate is influenced not only by the mean wind speed but also by wind turbulence characteristics and the pressure fluctuations at the opening. These factors must be understood and calculated when the airflow rate at the opening is in question.

In earlier work conducted by P.R. Warren in 1977, Warren researched turbulent convection of airflows through a single-sided opening in a building envelope. The core concept of his work is finding eddies that are the same size or smaller than the window size are the type of eddies that contribute to airflow through an opening. These findings were based on both full-scale buildings and wind tunnel experiments. Warren also found the incidence angle of the wind on an opening would change the airflow velocity obtained at the same opening. To simplify, wind velocity at the opening wouldn't only be affected by the reference wind velocity but also by the angle at which the wind is facing the opening in question. These findings were derived

from the observation that airflow pattern changes at an area of interest, e.g., opening, as a function of the wind incidence angle. [225]

In 1985, P.R. Warren and L.M. Parkins derived an expression to address the effects of wind on the airflow rate obtained at an opening. In this work, Warren and Parkins excluded the effects of temperature differences and the incident angle at which wind is facing an opening. Thus, the following expressions represent the airflow rate at the windward falling angle. [225]

$$Q_v = 0.1 \cdot U_L \cdot A \quad (2)$$

$$Q_v = 0.025 \cdot U_R \cdot A \quad (3)$$

3.2.3 The combined effect of buoyancy and wind velocity

In the aim to understand the influence of the combined effect of buoyancy and wind on a single-sided ventilation, research is limited due to the complexity of the matter. However, De Gids and Phaff conducted a notable full-scale experiment in 1982 that incorporated both these factors. [226]

Their study treated the complexity associated with determining the velocity profile at a single-sided opening, which depends on which of wind or thermal buoyancy is more dominant and, thus, considered the factor of being more influential on airflow rate obtained at the opening. The experiment was carried out at three urban locations with surrounding buildings up to 4 stories high. In their work, measurements were taken only on the first floor, and the data that were addressed and included are wind velocities as of reference and local, air changer rate, and temperature differences between indoors and outdoors. Those measurements amounted to 33 measurements in total with different scenarios. [226]

The following empirical expression was then derived for mean air velocity at the opening.

$$Q_v = A_{eff} \cdot U_L \quad (4)$$

$$U_m = \sqrt{0.001 \cdot U_R^2 + 0.0035 \cdot h \cdot \Delta T + 0.01} \quad (5)$$

A_{eff} describes the portion of an opening that actively contributes to the airflow into a space, .e.g., room. A_{eff} accounts for several factors such as opening geometry and type, e.g., sliding, skylight and casement, discharge coefficient, and airflow characteristics.

3.2.4 The combined effects of buoyancy, wind velocity, and direction

So far, buoyancy and wind velocity have been discussed homogenously and combined in terms of their contribution role on airflow rate obtained at an opening. The expressions derived allow designers of natural ventilation to understand how such effects can affect the air exchange rate obtained at the opening in question. Despite the following expressions from these studies being based on multiple, full-scale, and wind tunnel experiments, it does not reflect the complexity associated with real-life scenarios. These studies can give a fair accuracy to real-life measurements but were conducted using windward experiments. In real life, wind impacts buildings from different directions. Warren and Parkins understood the differences associated with such a dimension, but no further assessment was made in such a manner. T. Larsen and P. Heisenberg understood such complexity and conducted full-scale wind tunnel experiments to derive a more comprehensive expression to account for the wind direction and for the domination aspect of buoyancy and wind on their role of influencing the airflow rate obtained at an opening. [223]

To perform the experiments, Larsen and Heisenberg experimented on a constructed building with an opening in a wind tunnel experiments. The scale of the building was $[x,y,z] = 5.56$ meters, 5.56 meters, 3 meters and the opening was of 0.86 meters, 1.4 meters corresponding to an area of 1.2 m^2 and the room volume was 68.95 m^3 . During the experiments made, the model was rotated from 0 to 345 in increments of 15 or 30 where measurements were taken by each change of increment. The wind velocity was adjusted between 0, 3, and 5 $[\frac{m}{s}]$, while the temperature differences between the indoor and the outdoor of the model were 0, 5, and 10 $[C^\circ]$. A total of 159 different measurements were taken with different scenarios, and the air exchange rate was determined using a tracer gas decay method. [223]

Thereafter, the air exchange rate was evaluated by plotting the varying effects of wind velocities, temperature differences, and incidence angles. The incidence angle starts with 0, and it represents wind facing the opening; in a sense, it corresponds to experiments made by

Warren, Parkins, De Gids, and Phaff. It is observed that temperature differences significantly impact low wind velocities. This effect is most observed when the incidence angle is between 90-and 270. In such cases wind is flowing parallel to the opening. As wind speed increases, it was observed that air change converges, which shows a reduced effect of temperature differences on the resulting air change rate. [223]

It is then concluded, based on observations, that in isothermal conditions, higher wind velocity leads to a higher air change rate with nearly parallel curves. However, it is observed that the effects of wind velocity diminish when the flow is parallel to the opening. [223]

$$Q_v = \pm C_D \cdot A_{eff} \cdot \sqrt{\frac{2 \cdot |P_{wind} + \Delta P_{thermal} + \Delta P_{fluct}|}{\rho}} \quad (6)$$

$$Q_v = A \cdot \sqrt{C_1 \cdot f(\beta)^2 |C_p| \cdot U_R^2 + C_2 \cdot h \cdot \Delta T + C_3 \cdot \frac{\Delta C_{p,opening} \cdot \Delta T}{U_R^2}} \quad (7)$$

Direction	Incidence angle (β)	C_1	C_2	C_3
Windward	0-75° and 285-360°	0.0015	0.0009	-0.0005
Leeward	105-255°	0.005	0.0009	0.0160
Parallel flow	90° and 270°	0.001	0.0005	0.0111

Table 2: coefficient values corresponding to incidence angle β

3.3 CFD

By answering the first research question, it is now understood how thermal and wind conditions can change the airflow rate obtained at a single-sided ventilation. A pattern was identified in terms of a domination effect when both temperature differences and wind velocity assist the flow at an opening. It is also understood that wind direction can change the results concerning the dominating effect in question. The understanding derived that each case differs from another with regard to altering wind velocity and direction, and temperature differences between indoors and outdoors underlays that perhaps in the context of airborne transmission the results might or cannot be similar in each case. As mentioned earlier, temperature differences will not be considered in answering the second research question, and well-mixed air is assumed indoors and outdoors, but since thermal plume is taken into consideration, the kinetics of the results perhaps would be affected in terms of airflow rate.

Although, in this case, it is assumed that the wind would be the dominating effect over airflow rate obtained at the openings where airborne transmission is assumed to occur, in order to open the windows and allow the air to filtrate through these openings requires a conscious or unconscious action of the infected occupant to engage in opening the window. Such an aspect can occur if the infected occupant is feeling thermally dissatisfied with his/her surrounding thermal conditions. Hence, the importance of thermal plume in answering the second research question is highlighted. Thermal plume intensity is a dynamic aspect; factors that can change its intensity are understood to be a change in the metabolic rate of an individual. Revisiting lipid-enveloped viruses, Common symptoms of SARS-CoV-2 infection and other lipid-enveloped viruses is fever, also known as Pyrexia, which leads to a temporary increase in body temperature. To elaborate, a sick individual with a common respiratory illness would experience an elevation of body temperature than the normal range as a mechanism to fight the disease. [180] [181] In the context of thermal dissatisfaction, an occupant would feel dissatisfied then and engage in opening the window in question.

The process of answering the second question can be simplified by following the initial steps shown in Figure (4), which is a complete guidelines flow of a CFD modelling process [183]. Since the objective is explained, hence, the first step to answering the second research question is then to choose a place where such a phenomenon would occur. Thus, a location, building, and rooms shall be chosen. In the following thesis, U-huset was chosen as the building where the occurrence would happen.

U-huset or as referred to U-building, is a building located at the main campus of the Royal Institute of Technology “KTH” found in Stockholm, Sweden. KTH is one of Sweden’s leading technical universities that offer and is renowned for its engineering and technology programs. U-huset is a multifunctional facility, featuring lecture halls, classrooms, laboratories, and study rooms. Moreover, U-huset utilizes smart building technologies that enhance efficiency, sustainability, and occupant comfort.

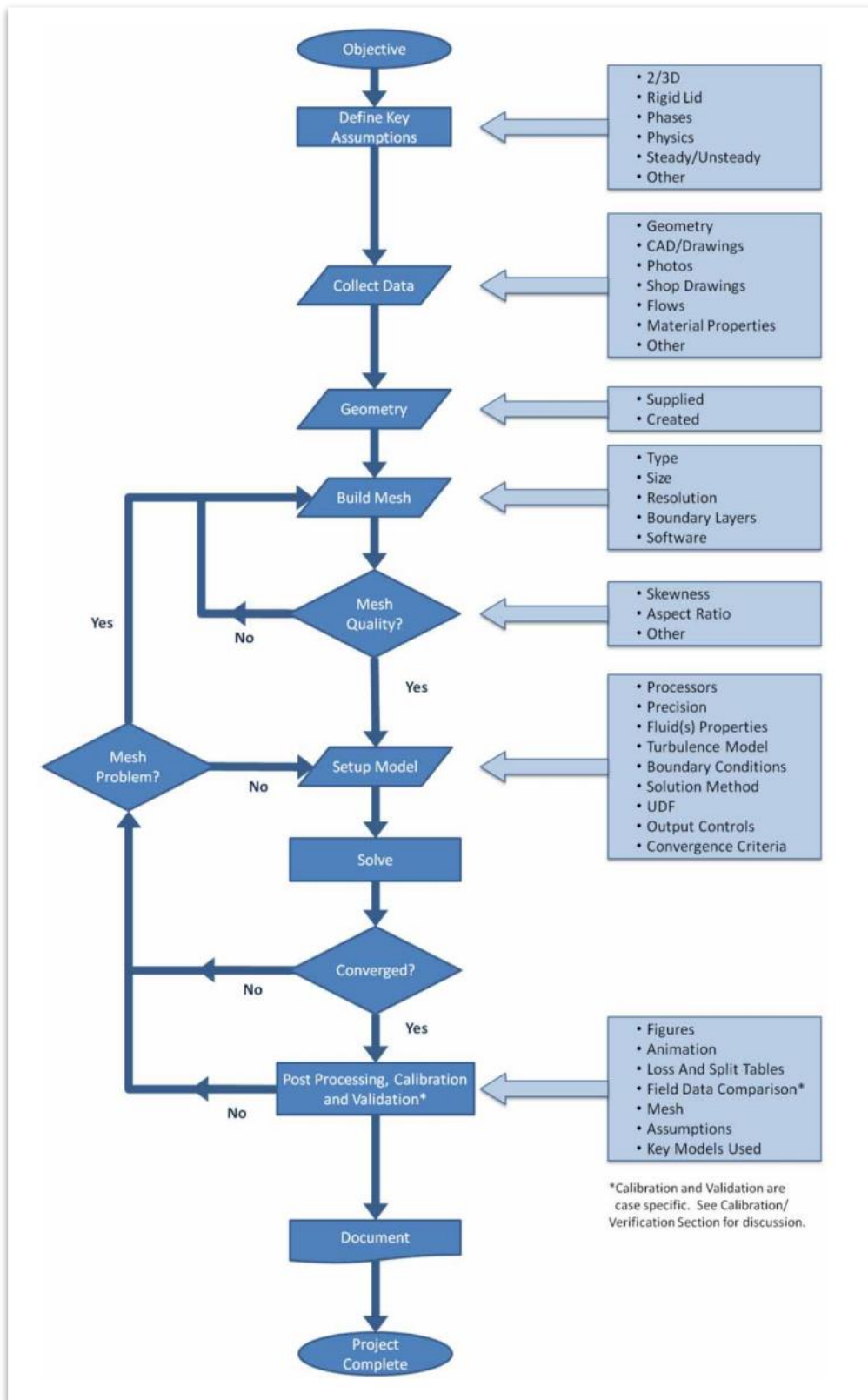


Figure 4: CFD process

Further, an assumption of the location where the sick occupant is located shall be identified. It is assumed, then, that the sick occupant is isolated in a nonshared space with others. Hence, the occupant would consider opening the window without taking into account other occupants to be thermally dissatisfied. Thus, the chosen room shall be small in volume where individuals can be located without others occupying the same space. Study room is a good fit in this case to be the room in question. U-huset offers 8 study rooms located perpendicular to each other in a set of 4 rooms. [182] 3 rooms were chosen in this case: 1 room parallel to the room where the sick occupant is located and 1 room perpendicular to that same room. Hence, perpendicular and parallel transmission can be examined. The rooms are located on the fourth and sixth floors of the building, with windows located close to each other. Next, following the guidelines, given in figure (4), Data collection is necessary to obtain space coordinates of the place in question. Hence, a virtual model designed in Revit given in the following course, “AF2513 - Smart buildings” at the Royal Institute of Technology was used to obtain the geometrical data of the rooms and the building. Refer to figures (5 and 6) for the model and the chosen rooms.

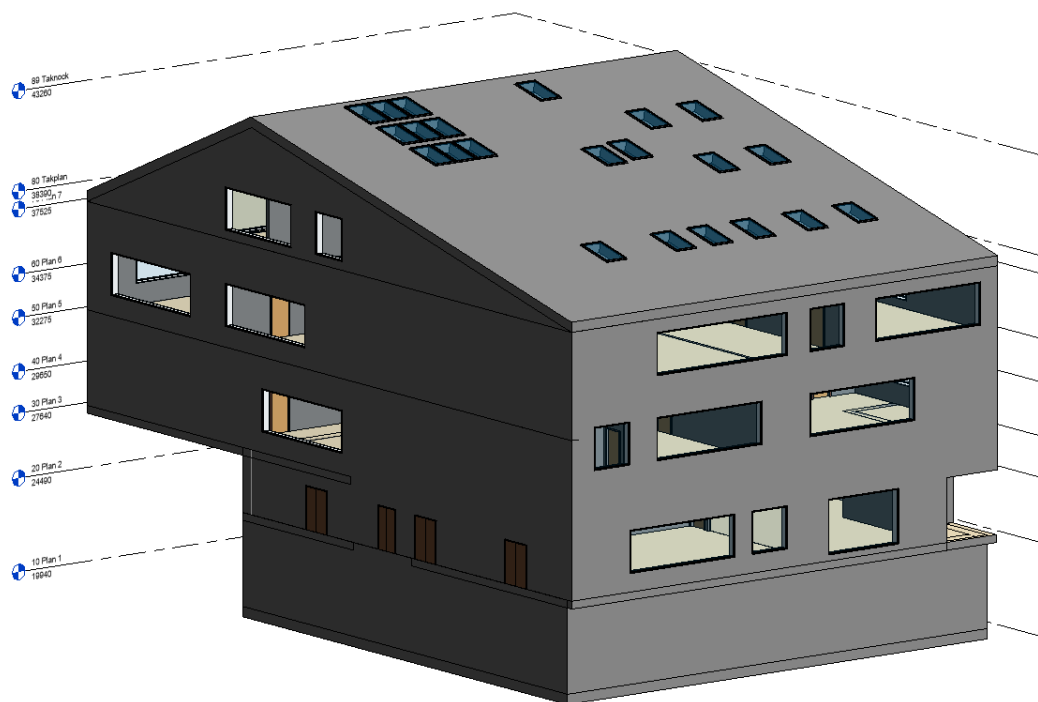


Figure 5: Revit geometry model of U-huset



Figure 6: floor 4 and 6 with the rooms of interest

Although such data was provided in the model, the accuracy of the model is still in question, thus, a manual confirmation of the geometries given in the model was performed. Such confirmation was made by manual measurements of spaces that are small and reachable, e.g., the Surface area of the rooms. For large and unreachable spaces, e.g., building walls, and room height, Lidar scanner was used on iPhone model 12 pro. Refer to appendix A.3 for accuracy evaluation of the scanning method. The difference between the geometries obtained from the model and the manual measurements was ± 5 cm. Upon that, the virtual model geometries were used as a reference. Refer to table (3) for the parameters: room names, opening size, room volumes, co-ordinational location, distance above ground, and room surface area.

Room	Opening size	Volume	Location	Distance to occupied room	Distance above ground	Surface area
	[m²]	[m³]		[m]	[m]	[m²]
434	0.7488	50.15	East wall	0	5.76	11.543
433	0.7488	50.15	East wall	4.6	5.76	11.543
634	0.7488	51.06	East wall	2.646	10.485	11.543

Table 3: description of rooms parameters; Opening size, volume, location, distance to occupied room, distance above ground and surface area

A slight disparity in volume can be observed in the room located on the 6th floor due to the parallel slope between the ceiling and the roof. The linear equation given in Appendix (A.4) was used to identify the corner coordination points needed to build the room geometries and further assess airborne transmission.

3.3.1 Overview of ICEM

Ansys ICEM was used to build the geometries and meshing processes. Ansys ICEM is software provided by ANSYS that provides meshing and pre-processing capabilities. The software provides tools for generating various types of meshes, including structured, unstructured, hybrid, and hexahedral meshes. Along with the easy user-friendly interface that facilitates the definition and control of meshing parameters, users can import geometries from CAD software in different extensions, e.g., IGS, STP, PRT, and STL. Another benefit of using ICEM is the seamless integration with CFD Solvers. [185]

The overall process of generating a mesh can be seen in figure (7) [190].

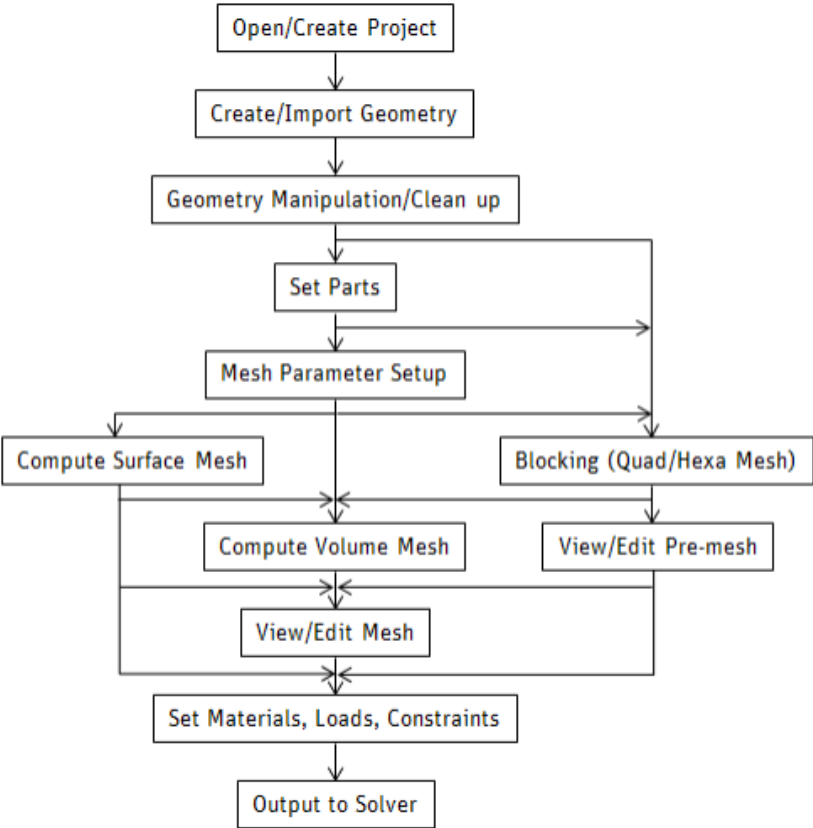
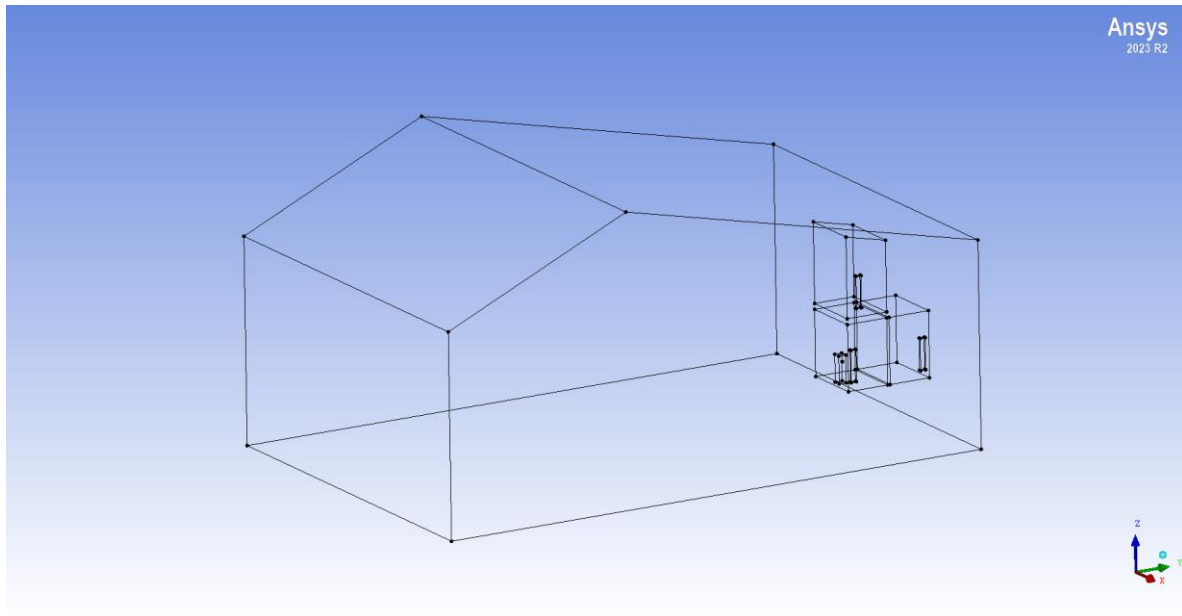


Figure 7: ICEM process

3.3.1.1 Geometry setup

Following, the geometries were exported with the extension STL and imported to ICEM where the points that define each edge were identified and created.



Figur 8: ICEM building geometry

Extra attention was paid to have all points creating a surface to be on the same plane. To elaborate, the two points highlighted in figure (9) exist in the same plane in the coordinates y and z . Likewise, all the points were confirmed to carry the same principle. The following assures no having any gradients in the building envelope which improves the accuracy of the results once calculated. A slight displacement of 12 cm was assigned to the windows. This act is important to avoid having a 2d surface where surface meshing might cause a problem in transitioning between indoor and outdoor walls.

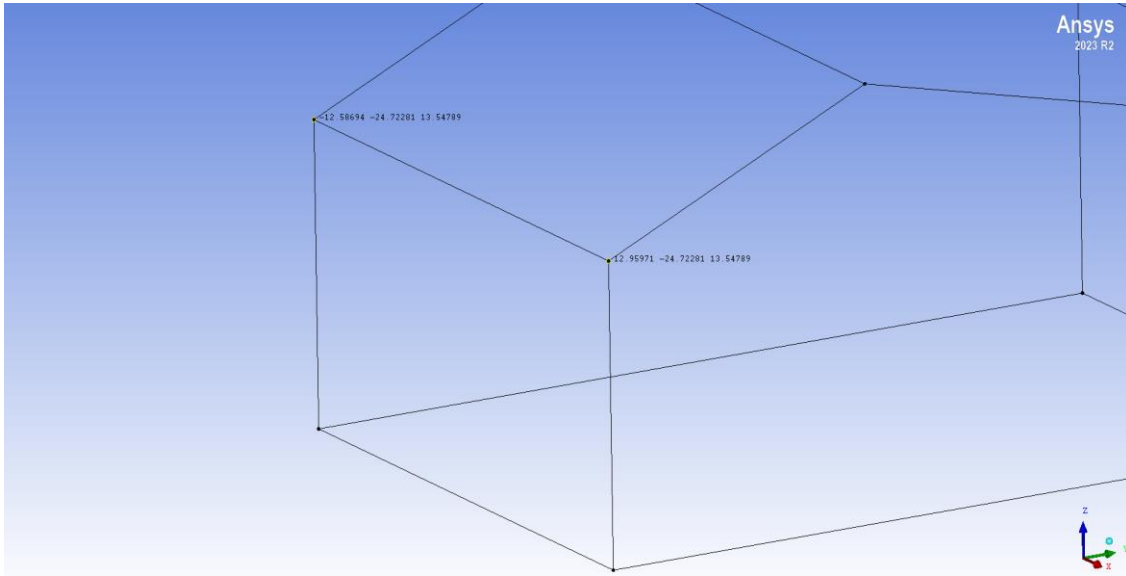


Figure 9: Dimensional matching in coordinates on the same plane

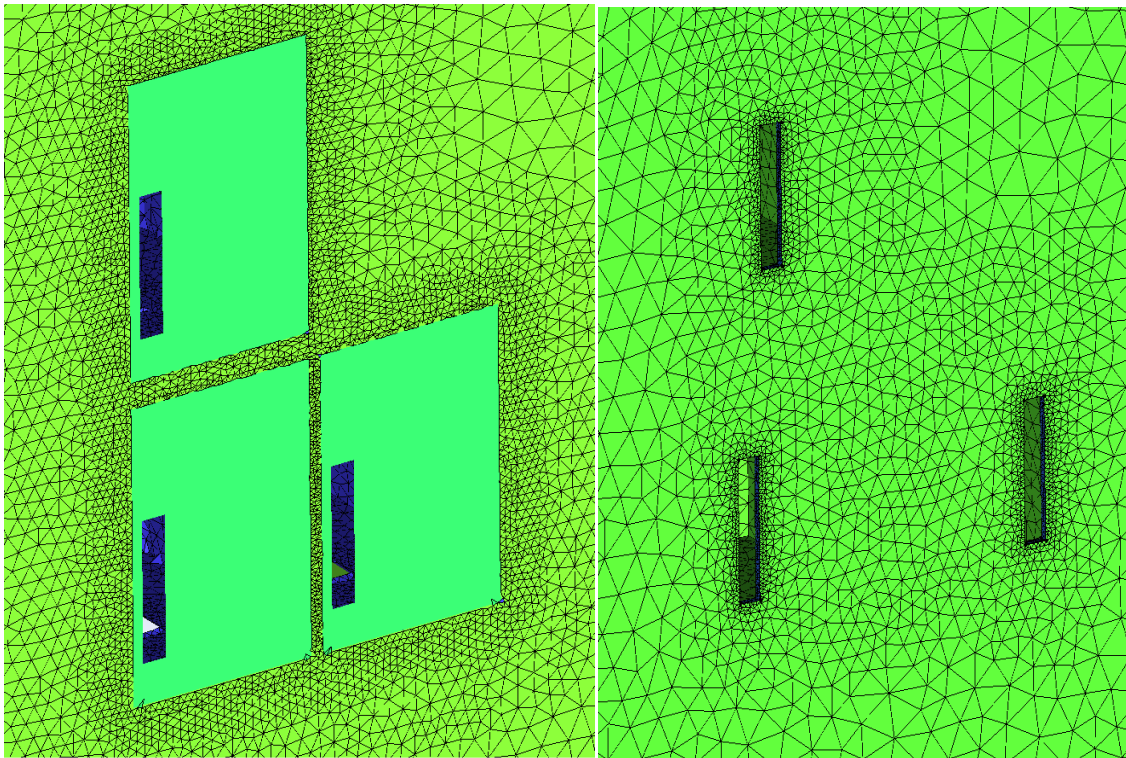


Figure 10: 2D mesh disturbance

Adopted 3d thickness to windows

Next, a dispersion model mimicking a human was generated using an average human height 1.7 m and mouth size of 4 cm² [186]. Next, since the objective includes natural convection, guidelines were analyzed to understand the domain size needed to predict the flow at the building. the guidelines for the CFD build-up were proposed by the Working Group in the Architectural Institute of Japan “AIJ” which aligns with the recommendation of the European Cooperation in the field of Scientific and Technical Research “COST”, Group (Action C14 “Impact of Wind and Storms on City Life and Built environment” Working Group 2 – CFD techniques) [187] [188] [189]. The guidelines can be summarized as the following for the domain size.

<i>Domain size</i>	Recommended Length “AIJ”	Recommended Length “COST”	Chosen Length
<i>Top boundary</i>	5H	5H	5H
<i>Lateral boundary</i>	5H	2.3W	5H
<i>Inlet boundary</i>	5H	5H	5H
<i>Outlet boundary</i>	10H	15H	15H

Table 4: chosen dimension for the domain size

The outlet boundary was set to 10H at first, then increased to 15H as an issue was occurring at the outlet boundary when only natural convection simulation was held. Further, the quality of the geometries was checked using building diagnostic topology feature in ICEM. The built domain and the geometries check can be seen in Figure (11), where “red” is a code of good metrics for the geometries.

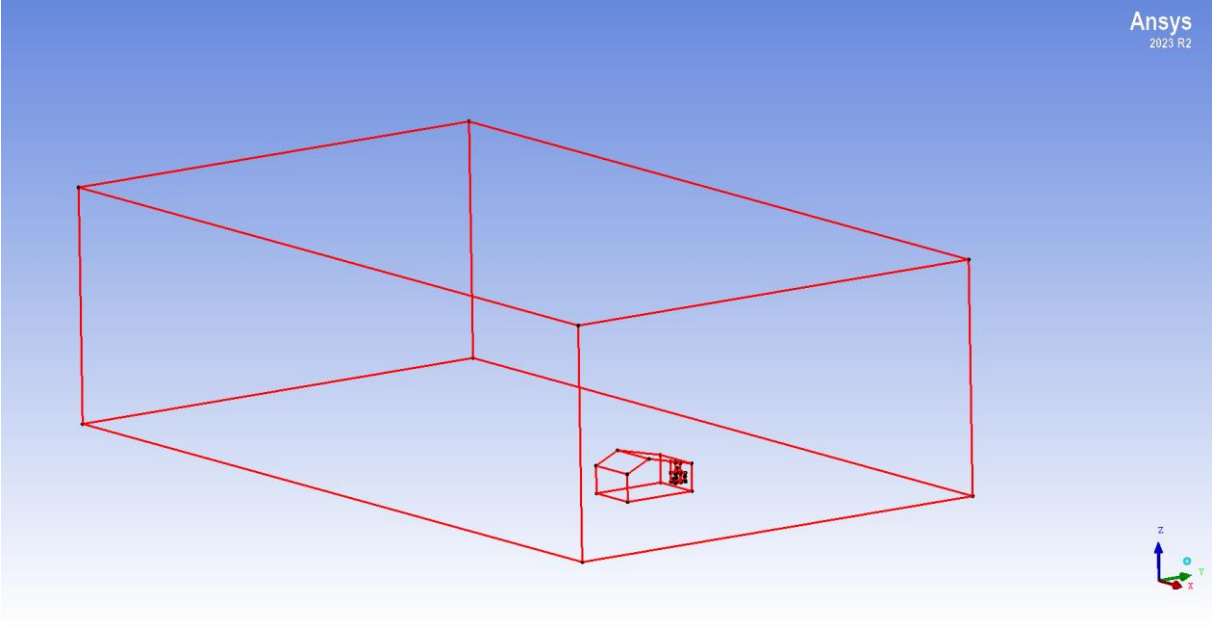


Figure 11:Diagonstic topology

Next, surfaces were built and assigned to parts. According to “AIJ”, a blockage ratio should be below 3% to avoid interference in wind flow measurements. With the chosen value for the domain size, a blockage ratio of less than 2% was obtained for this model.

3.3.1.2 Grid setup

In terms of grid setup, AIJ recognizes the problem with flow at the edges of the building. Thus, a recommendation of a finer grid arrangement at the corners is made to resolve the flow near the corners. Subsequently, a minimum of 10 grids is required on one side of a building to capture separation flow around the upwind corners accurately, for the following a grid resolution of between 0.5-5 meters would then achieve the outcome needed. Further into the recommendations, a stretching ratio of no more than 1.3 should be assigned for the elements. Higher stretching ratios were found to cause a problem with the quality of the mesh for parts with different maximum sizes in the same regions. It is preferred to use unstructured mesh in order to improve the accuracy of the results obtained. It is necessary to mention that all of the grid setup recommendations of AIJ are aligned with COST. [187]

Upon analyzing the following recommendation, the values were used as a part mesh setup. For indoors, a maximum size was set to 0.3m and 0.001m for the occupant's mouth to capture the small details when cough dispersion occurs. Upon the recommendations, the surface mesh at the corners was set at 0.1m, and the maximum global element size was allowed to stretch to 32.

Part	Prism	Hexe-core	Maximum size	Height	Height ratio	Num layers	Tetra size ratio	Tetra width	Min size limit	Max deviation	Prism height limit factor	Prism growth law	Internal wall	Split wall
ASCII	<input type="checkbox"/>	<input type="checkbox"/>		0	0	0		0	0	0	0	undefined	<input type="checkbox"/>	<input type="checkbox"/>
BETWEEN_INDOOR_AND_OUTDOOR	<input type="checkbox"/>	<input type="checkbox"/>	0	0	0	0	1.3	0	0	0	0	undefined	<input type="checkbox"/>	<input type="checkbox"/>
CREATED_MATERIAL_39	<input type="checkbox"/>	<input type="checkbox"/>										undefined	<input type="checkbox"/>	<input type="checkbox"/>
EAST_WALL	<input type="checkbox"/>	<input type="checkbox"/>	0.8	0	0	0	1.3	0	0	0	0	undefined	<input type="checkbox"/>	<input type="checkbox"/>
INLET	<input type="checkbox"/>	<input type="checkbox"/>	0	0	0	0	1.3	0	0	0	0	undefined	<input type="checkbox"/>	<input type="checkbox"/>
NORTH	<input type="checkbox"/>	<input type="checkbox"/>	0	0	0	0	1.3	0	0	0	0	undefined	<input type="checkbox"/>	<input type="checkbox"/>
NORTH_WALL	<input type="checkbox"/>	<input type="checkbox"/>	0.8	0	0	0	1.3	0	0	0	0	undefined	<input type="checkbox"/>	<input type="checkbox"/>
OCCUPANT	<input type="checkbox"/>	<input type="checkbox"/>	0.3	0	0	0	1.3	0	0	0	0	undefined	<input type="checkbox"/>	<input type="checkbox"/>
OCCUPANT_MOUTH	<input type="checkbox"/>	<input type="checkbox"/>	0.001	0	0	0	1.3	0	0	0	0	undefined	<input type="checkbox"/>	<input type="checkbox"/>
OUTLET	<input type="checkbox"/>	<input type="checkbox"/>	0	0	0	0	1.3	0	0	0	0	undefined	<input type="checkbox"/>	<input type="checkbox"/>
ROOF	<input type="checkbox"/>	<input type="checkbox"/>	0.8	0	0	0	1.3	0	0	0	0	undefined	<input type="checkbox"/>	<input type="checkbox"/>
ROOMS	<input type="checkbox"/>	<input type="checkbox"/>	0.3	0	0	0	1.3	0	0	0	0	undefined	<input type="checkbox"/>	<input type="checkbox"/>
SKY	<input type="checkbox"/>	<input type="checkbox"/>	0	0	0	0	1.3	0	0	0	0	undefined	<input type="checkbox"/>	<input type="checkbox"/>
SOUTH	<input type="checkbox"/>	<input type="checkbox"/>	0	0	0	0	1.3	0	0	0	0	undefined	<input type="checkbox"/>	<input type="checkbox"/>
SOUTH_WALL	<input type="checkbox"/>	<input type="checkbox"/>	0.8	0	0	0	1.3	0	0	0	0	undefined	<input type="checkbox"/>	<input type="checkbox"/>
STREET	<input type="checkbox"/>	<input type="checkbox"/>	3	0	0	0	1.3	0	0	0	0	undefined	<input type="checkbox"/>	<input type="checkbox"/>
WEST_WALL	<input type="checkbox"/>	<input type="checkbox"/>	1	0	0	0	1.3	0	0	0	0	undefined	<input type="checkbox"/>	<input type="checkbox"/>

Show size params using scale factor
 Apply inflation parameters to curves
 Remove inflation parameters from curves
Highlighted parts have at least one blank field because not all entities in that part have identical parameters

Apply Dismiss

Figure 12: Part mesh setup

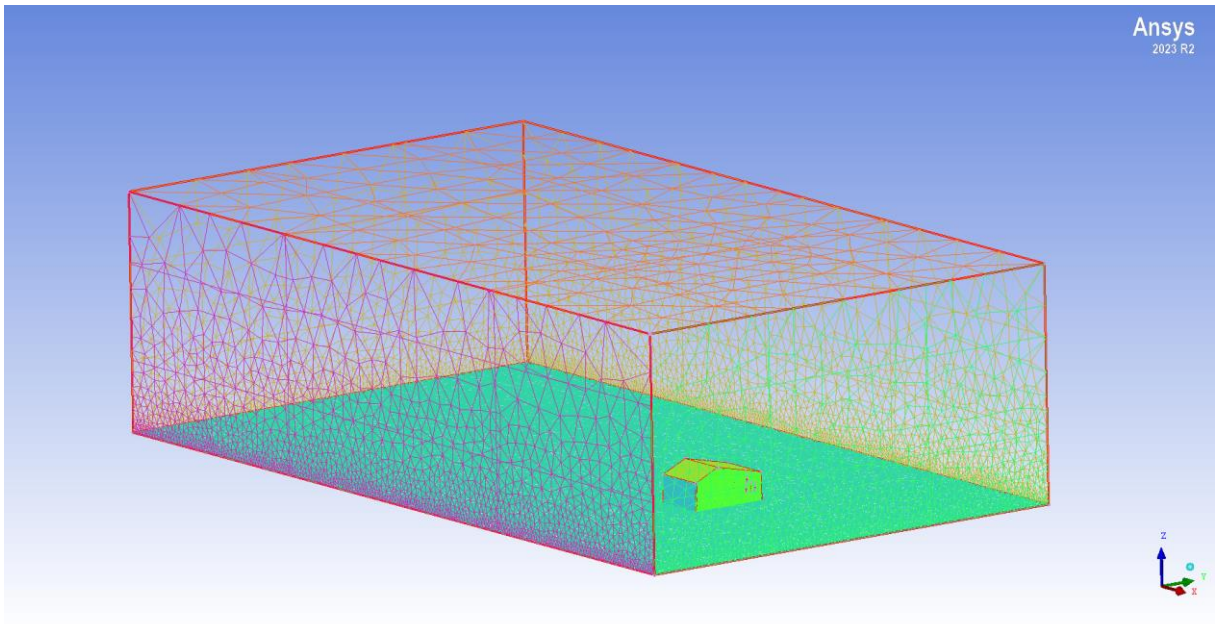


Figure 13: obtained domain mesh

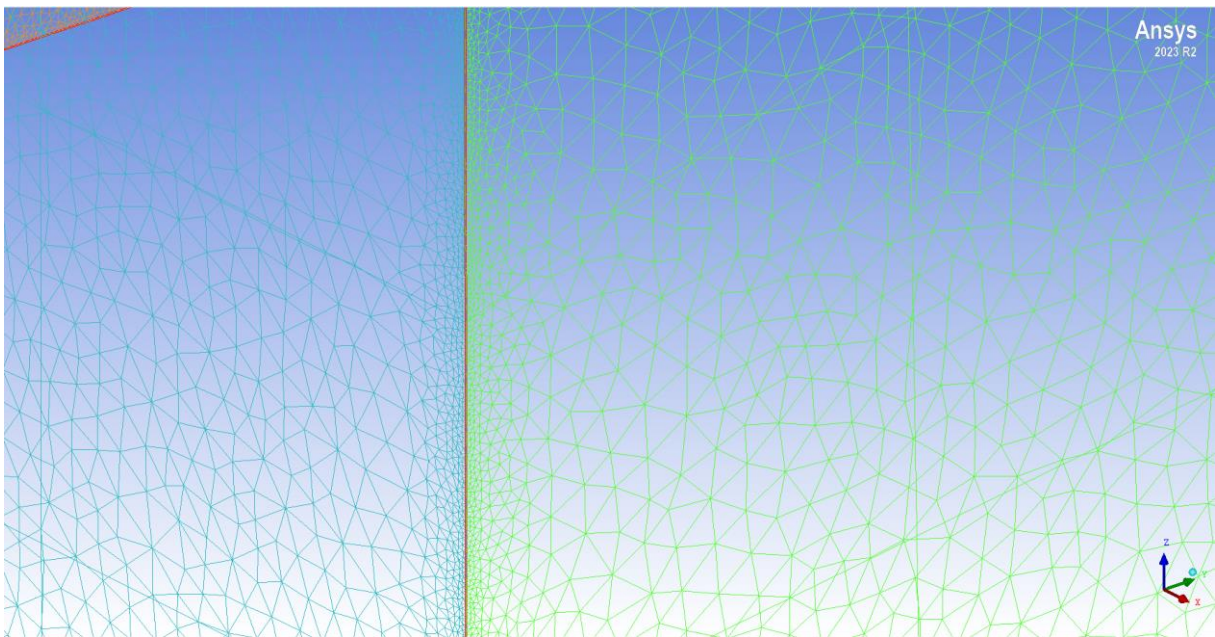


Figure 14: Finer mesh at the corners of the building

3.3.1.3 Grid elements count and quality

Upon following the process given in figures (4 and 7), the quality of the mesh was controlled in terms of skewness, aspect ratio, and overall quality, and the following was observed from the Display mesh quality function in ICEM. To elaborate on the findings, the X axis displays the quality of the mesh where, for such a case with natural convection, the aspect ratio, overall

quality, and skewness should be above 30%. As observed in the figures (15 and 16). The Y-axis represents the number of elements at which their quality corresponds to quality metrics. Moreover, the total grid elements for the following model were 2.3 million, and the total nodes were 0.42 million.

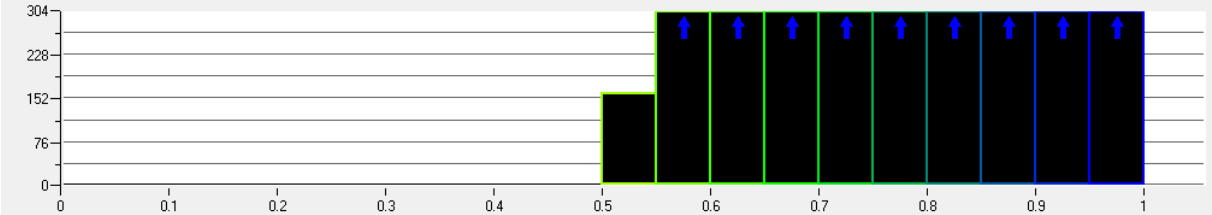


Figure 15: Skewness mesh quality

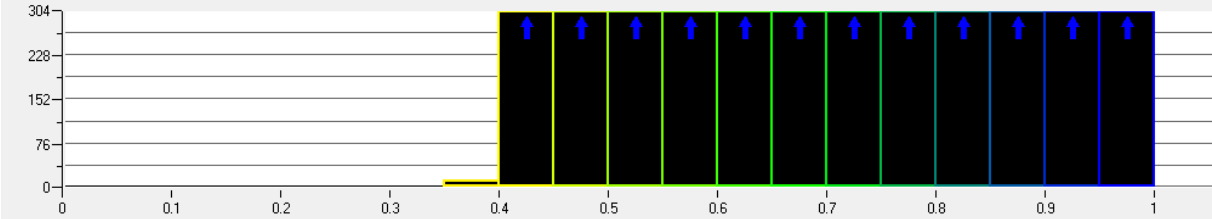


Figure 16: ratio and overall mesh quality

3.3.2 Overview of Ansys Fluent and turbulence engineering

The next step in obtaining results is choosing a solver. Thus, Ansys Fluent was selected to meet the objective studied in this thesis. First, Ansys fluent must be defined to understand how the software is used. Ansys Fluent is powerful Computational Fluid Dynamics software that is widely used by engineers and researchers due to its ability to simulate extensive physical models for complex geometries. The software features a user-friendly interface and can model both laminar and turbulent flows, multiphase flow, heat transfer, and chemical reactions. Ansys fluent offers parallel processing, which enables simulations to run on a cluster of processors. Thus, computational time can be reduced significantly. Fluent allows its users to customize specific algorithms when modeling a specific aspect through the use of User-Defined-Functions “UDFs.” The following can be achieved by translating a mathematical equation e.g., Velocity and temperature Profiles. A function written in C programming language that can then be computed in the software. Favorably, Ansys fluent manual provides its users with tutorials on how such a task can be executed. Further, turbulence modelling is crucial for simulating fluid flows. Hence, the three primary turbulence modelling approaches that can be used in Fluent are Reynolds-averaged Navier-Stokes “RANS”, Large Eddy Simulation “LES”, and Detached Eddy simulation “DES”. The choice of turbulence modelling rests on many aspects and depend on the objective that is being studied. To break down each of the turbulence modelling choices, one must understand the advantages and limitations of these turbulence modelling choices. Starting off with LES which can be explained as a turbulence modelling choice that resolves the larger, energy-containing eddies while offering a modelling of the smaller eddies that often occur next to wall boundaries. LES can be used in flow problems that have significant large-scale turbulence where detailed information is necessary to model. Thus, the following turbulence model is suitable for modelling large-scale atmospheric and oceanic flows where large eddies dominate and are necessary for the case studied. LES requires moderate computational resources due to its ability to obtain an accurate representation of large-scale eddies. RANS however, Split into steady and unsteady Reynolds-Averaged Navier-Stokes modulation “RANS” and “URANS” respectively. RANS modelling is used in cases where time-averaged information is sufficient to model a flow. The aforementioned modelling choice is suitable for applications where, High Reynolds number flows are dominating within a region of the domain that is important for the study conducted. Thus, the following turbulence model is

suitable in situations with complex geometries and high Reynolds numbers. Such an approach is common in industrial applications such as aero- and hydrodynamics evaluation, e.g., automotive design, renewable wind turbine design, and flows around a building. URANS Refers to the same modelling choice but is suitable for applications where unsteady and dynamic flow behaviours are crucial for the study conducted. Thus, better computational resources are required e.g. Bridge designing and transient wind loads.

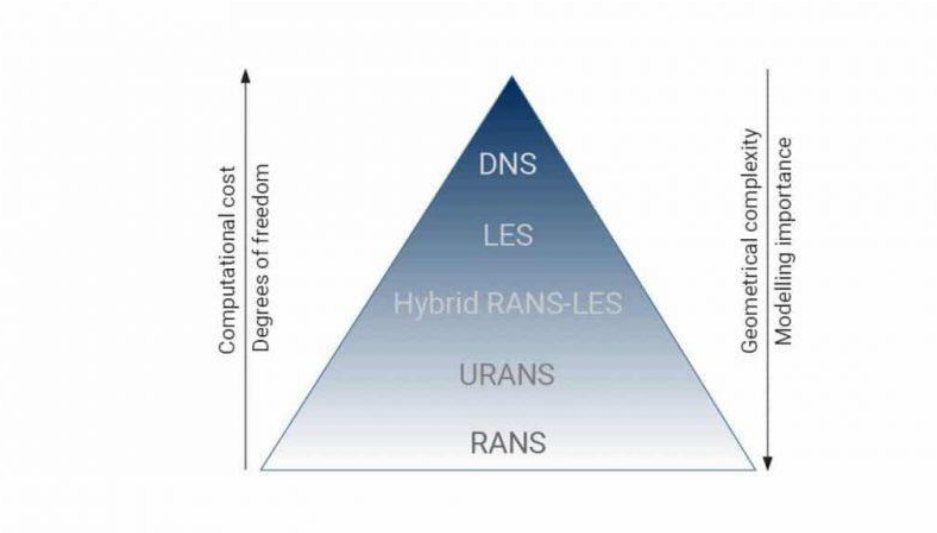


Figure 17: description of turbulence modeling in terms of computational cost, degree of freedom, geometrical complexity and modelling importance

In both cases, turbulence effects are required to be solved with additional equations referred to, turbulent kinetic energy “k” and its dissipation rate “ε”. Both these additional equations will be further explained upon the choice of the turbulence model. The last modelling choice is referred to as DES, and implies a hybrid method that combines both elements of RANS and LES. To understand, this modelling choice uses RANS approach in near-wall regions and LES in freestream regions. The aim of this modelling choice is to be used in a context where a detailed understanding of turbulence is required and is suitable for low Reynold numbers due to its ability to capture detailed flow. Thus, highly accurate numerical results can be achieved on behalf of extreme computational resource requirements. [212]

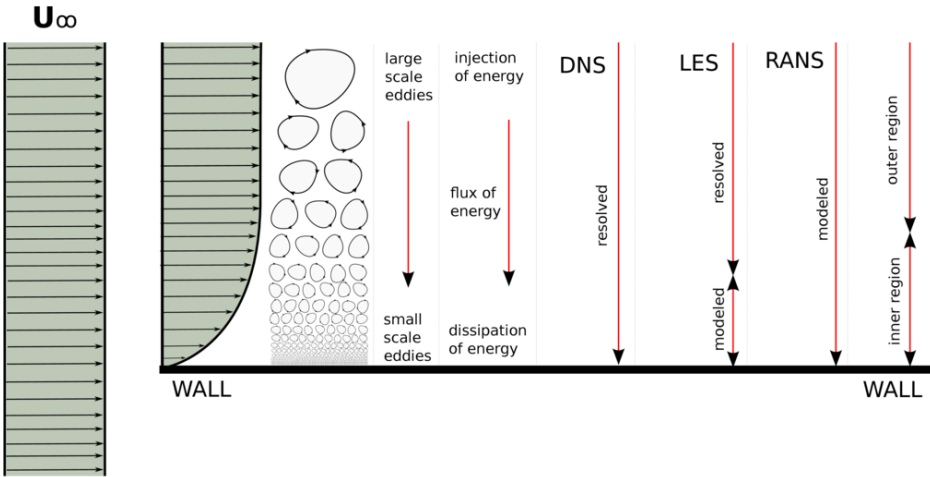


Figure 18: Turbulence modelling approach in near wall treatment

3.3.2.1 Wind

As mentioned, to meet the objective of this study, natural convection is one of the phenomena that should be understood to recognize how wind behaves next to and away from a boundary layer. To make sense of it, fluid behavior needs to be understood when stress is applied. Fluid is defined as a substance that exists in one of the following states, liquid or gas. Unlike solids, fluids cannot resist an applied shear stress without deforming continuously. Thus, a mean difference between solids and fluids is the ability of solids to withstand an applied tangential force until reaching a certain strain angle. In contrast, the same stress applied to a fluid is proportional to the rate of strain. Hence, a fluid will keep on deforming and achieve a constant strain rate until the force is lifted. [214]

Wind is a prime example of a fluid in motion and air is considered the mean medium of natural convection. Hence, understanding the behaviour of fluids when shear stress is applied helps with analyzing how wind moves about and interacts with its surrounding environment, e.g., buildings, trees, and automotive. At first, such interaction considered to be an external flow in the examples mentioned above, the fluid e.g. air in this case is in motion and the object can either be stationary or in motion. Despite the apparent difference from an observer's perspective, both objects, stationary and in motion, are equivalent as relative motion between air and the object is the key factor. [214]

However, a simplification of how air behaves when encountering objects cannot be made due to the influence of the body's shape on the flow characteristics. Hence, in fluid dynamics, bodies can be simply categorized as aerodynamic or bluff bodies. To understand the difference in flow characteristics over such bodies, two concepts should be introduced. These two concepts are referred to as drag and lift forces. Given air as the medium of interest in this following study, when wind streamlines encounter an object, it exerts pressure forces acting normal to the object's surface and shear forces acting tangential to the same object's surface due to the viscosity of the fluid. [215] These forces exerted on the object's surface give rise to drag in the direction of the wind streamlines and lift perpendicular to the object's surface. These forces magnitude depends on various factors. These factors include fluid density, velocity, body size, shape, and orientation. Thus, air characteristics past the object would be influenced by a-symmetrical shapes. Since deriving an expression of these forces is rather challenging due to the complexity and nonlinearity of the fluid flow, two empirical relationships often used by engineers and scientists can quantify these forces. Drag and lift

coefficients are used in such a manner. [215] These coefficients are dimensionless and depend on the fluid density, the velocity of the fluid relative to the body, and the frontal area of the body at which the fluid is facing. In the building environmental sector, such an area is referred to as the windward area. The importance of these coefficients arises differently in the engineering application in question. To understand, In designing airfoils, it is crucial for the geometries and the shape of the airfoil to generate as much lift force and minimize the drag force exerted on the airfoil by the fluid. Such a design thus would emphasize a greater lift for the foil to withstand its mass at a lower kinetic energy. This design often exhibits the characteristics of a smooth and streamlined design. Unlike airfoils, buildings are considered to be bluff bodies with sharp corners; thus, in such a scenario, lift forces are less of an important aspect, and the drag force is more critical. To grasp the aforementioned statement, drag forces are a crucial aspect to be aware of in building designs where the objective is for the building to withstand environmental factors such as wind load calculations. However, lift forces are less of a concern in building designs other than providing critical information on the uplift forces of the roof. Since both drag and lift forces depend on the velocity and density of the fluid, thus these forces are considered functions of the Reynolds number. The following mainly arises from the fact that the Reynolds number characterizes the flow regime of the fluid, e.g., Laminar and Turbulent. The way to understand the previous statement is perhaps by defining Reynolds number. Thus, Reynolds number “Re” can be explained as a dimensionless measure between inertial forces to viscous forces in the fluid. Thus, it indicates the flow regime of a certain fluid. Laminar flow typically occurs when $Re \leq 2000$. Whereas turbulent flow occurs when $Re \geq 4000$, and the greater the Reynolds number is, The more chaotic the flow gets with vertices and eddies creation. [215]

3.3.2.1.1 Windrose analysis

Delving deeper into the analysis, we've come to grasp the significant impact of lift and drag forces on the formation of eddies, and how these phenomena alter airflow around buildings. It's evident that factors such as the angle and magnitude of wind impact play crucial roles in shaping these forces. Consequently, windrose analysis emerges as a vital tool for determining the angle of wind impact and its orientation relative to the building, thereby identifying key force parameters affecting the building which then affect the airflow around the building. Windrose analysis is a method widely employed in meteorology and environmental studies

and offers valuable insights into the wind characteristics at a specific location over a defined period. This analytical approach involves visually representing the frequency and direction of winds observed at the site. By plotting wind data comprising direction and speed onto a circular diagram, the analysis calculates the frequency of each occurrence and depicts it through varying lengths and color codes within corresponding segments. This method unveils prevailing wind patterns, dominant wind directions, and fluctuations in wind speed, thereby aiding in the identification of relevant scenarios for the study. [216]

Upon examining Figure (19), a distribution analysis across 16 directions is observed with each spanning a 22.5° increment change in angle. The length of each arrowhead in the figure indicates the frequency of wind hitting at the respective angle. These observations were derived from data collected over a decade at Stockholm's weather station, with information gathered on an hourly basis. Further into the analysis, the head length is divided into segments with the corresponding wind magnitude observed in each direction. Examining wind magnitudes more closely, a wind class is derived with a frequency distribution of each class occurrence over the same set of time of data collection. Hence, an observation was made on the West being the most dominating direction from which wind comes. Further, Southeast and northwest are the next dominating directions. Furthermore, the dominating wind magnitudes are observed to occur between 0.5-5.5 m/s where it makes 73.3% out of the total wind magnitudes observed over 10 years period. [217]

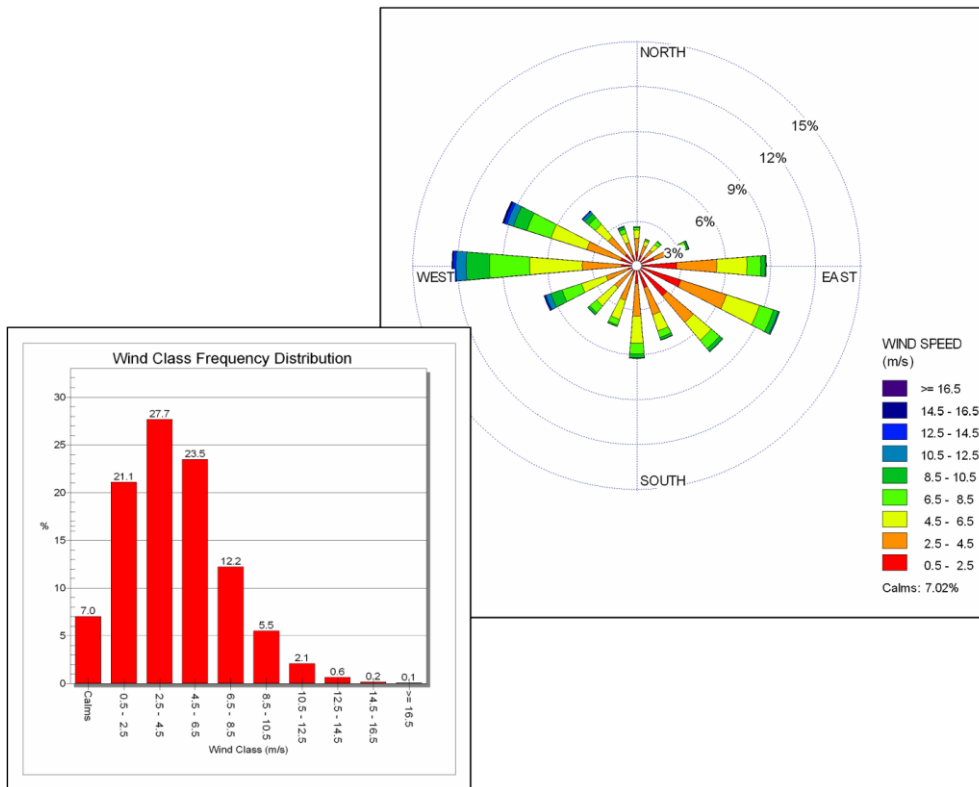


Figure 19: Windrose and wind velocity frequency distribution

Based on the observations made, limiting the study to only the dominating wind direction would be sufficient for the study; however, since the building doesn't respect symmetry upon its three-dimensional coordinates, it is favourable to examine all wind directions since each would perhaps lead to different results. The possibility of such examination is possible, but due to the limited computational resources, it is thus preferred to analyze the wind direction in increments of 45° instead, which reduces the cases from 16 to 8. Moreover, since wind magnitudes between 0.5-5 m/s made the a great portion of all wind magnitudes, 2 falls were considered at 2 m/s and 4 m/s. Thus, the total number of models to analyze is 16 in total, where 8 represent different wind directions, and for each, two wind magnitude cases can be analyzed. Through such an analysis, we would thus examine if altering wind magnitude would derive the same observation of particulate matter movement between the neighboring windows made in all the cases with different wind directions. [217]

3.3.2.1.2 Wind turbulence engineering

When considering modelling natural convection, the domain had to obey certain conditions, as mentioned in chapter (3.3.1). Thus, the following study addresses a wind flow over a flat plate representing the domain's ground surface. Bearing in mind the previous statement, it is necessary to understand the air velocity change with respect to the change in distance from the first fluid adjacent layer. Since no-slip condition is implied at the ground boundary, the velocity of the first layer adjacent to where the wind direction is parallel to, would be zero. This immobile layer thus would reduce the speed of the next layer due to friction and the following declaration would continue through the successive layers. The effect of the plate is felt up to a certain distance δ , where the free-stream velocity would remain nearly unchanged. Simplifying the problem to 2 dimensions, the x-component of the free-stream wind velocity u varies from 0 at $y=0$ to approximately 99% of u at $y=\delta$ as seen in figure (20). The following region is referred to as the velocity boundary layer, and within this region, four different subregions can be identified. These subregions are the viscous sublayer, buffer layer, overlap or logarithmic sublayer, and outer layer. The viscous sublayer is identified as the very first thin layer next to the wall where the viscous effects dominate. The flow is referred to be linear in that region. Further, the next layer is referred to as the buffer layer, and in this sublayer, both viscous and turbulent effects are significant. Above the buffer layer, where the turbulent effects are more dominant lays the logarithmic sublayer. The last sublayer in the velocity boundary layer would then be the outer layer where the turbulence effect dominates, and the velocity profile would thus match the free-stream velocity of the fluid, in this case, wind.

[215]

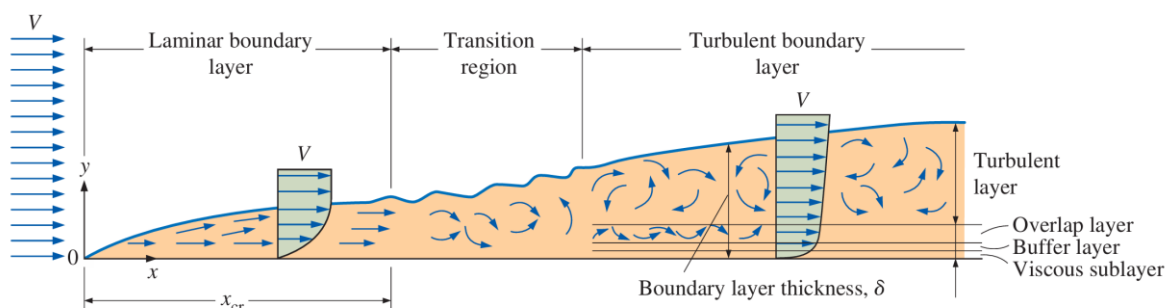


Figure 20: the boundary layer sublayers

To be able to resolve the objective of the second research question, modelling the near-wall flow eddies is important. Thus, one must trace down to the 1930s, when a Hungarian mathematician, Theodore von Kármán, identified recurring behavior patterns in the boundary layers across various scenarios. The following led to the formulation of the Law of the Wall. This law utilizes non-dimensional flow variables such as velocity “u” and distance from the wall “y” through the following empirical relations referred to as y^+ and u^+ as seen in equation 8 and 9. [215]

$$u^+ = \frac{u}{u_\tau} \quad (8)$$

$$y^+ = y \frac{\rho u_\tau}{\mu} \quad (9)$$

Here, u_τ represents the friction velocity and depends on the density of the fluid “ ρ ” and wall shear stress “ τ “. Shear stress is crucial for wall treatments since the velocity at the wall itself is zero due to the no-slip condition.

$$u_\tau = \sqrt{\frac{\tau}{\rho}} \quad (10)$$

These non-dimensional variables u^+ and y^+ , often termed "wall units," facilitate the comparison and extrapolation of physical quantities across different boundary layers. When examining the velocity profile in a boundary layer using wall units, one can distinguish three empirical relations describing the sublayers mentioned earlier. The relations mentioned below give the relation for modeling these non-dimensional flow variables.

$$u^+ = y^+ \quad (11)$$

$$u^+ = \frac{1}{\kappa} \text{Log } E y^+ + C^+ \quad (12)$$

Relation (11) is the linear region next to the wall where $y^+ < 5$. Whereas the relation given in (12) addresses the logarithmic sublayer where $(30 < y^+ < 300)$. Since in the buffer layer, both viscous and turbulence effects dominate, and it assesses the transition from linear to logarithmic profiles without governing law, modelling turbulence in this region is rather challenging. In Figure 21, one can identify how DNS turbulence model and Spalding wall function resolve this region, including the buffer layer. [222]

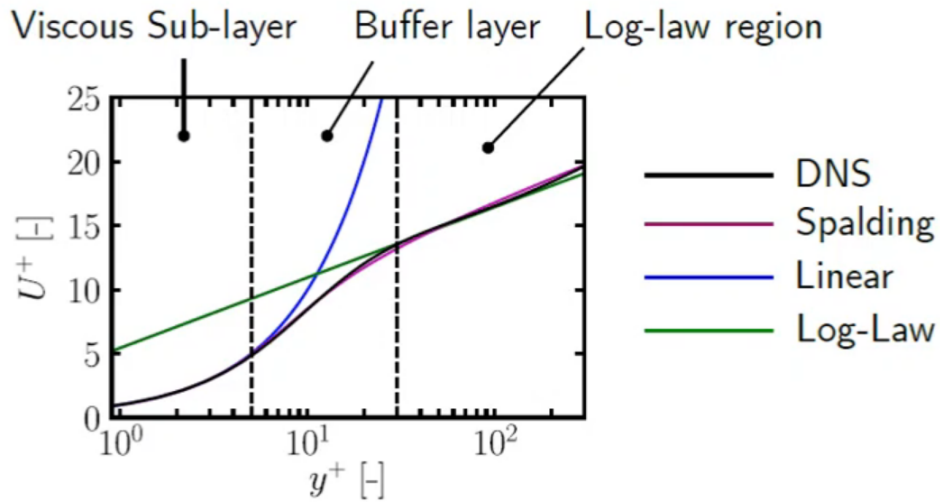


Figure 21: Near-wall region sublayers

Since the flow is required to be resolved in these regions to accurately represent flow separation and small eddies in these regions, one can notice that the first mesh layer should fall under the viscous sublayer. This aspect is possible, but it requires an advanced computational resource since resolving the flow in the viscous sublayer would require y^+ to be less than 5. Mainly, by looking at the relation (10) where the friction velocity tends to get higher due to its relation to shear stress, which increases the closer the flow is to the boundary, it is then noticed that the distance of the first layer from the wall would tend to 0. Such an arrangement would require a very thin height of the first surface mesh layer. Thus, a higher computational resource is required. [222]

3.3.2.2 Turbulence modeling and governing equations

Upon specifying the differences and limitations of turbulence models and deriving an understanding of near-wall regions in both chapters (3.3.2 and 3.3.2.1.2), DES and LES are excluded from turbulence choices for modeling the flow of the objective. The reason lies mainly behind the limited computational resources. Therefore, RANS would be significant enough to meet the objective studied. For incompressible turbulent flow, the instantaneous velocity field can be decomposed to its mean (time-averaged) component and a fluctuating component using Reynold decomposition as seen in equation (13). The same principle is applied for decomposing the pressure field as seen in equation (15). [221]

$$u_i = \bar{u}_i + u'_i \quad (13)$$

$$\bar{u}_i = \frac{1}{\Delta t} \int_t^{t+\Delta t} u_i dt \quad (14)$$

$$p = \bar{p} + p' \quad (15)$$

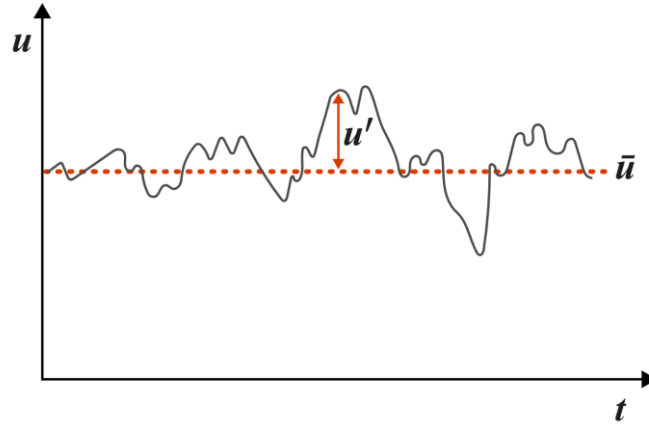


Figure 22: instantaneous velocity decomposition

When these decompositions are substituted and time-averaged into the instantaneous Navier-Stokes equations, which consist of a continuity equation representing the mass conversation principle and the momentum equations representing the conservation of momentum, as seen in equations (16) and (17), respectively, the Reynolds-averaged Navier-Stokes equations are then obtained as seen in equations (18) and (19). [221]

$$\frac{\partial(u_i)}{\partial x_i} = 0 \quad (16)$$

$$\frac{\partial u_i}{\partial t} + u_j \frac{\partial u_i}{\partial x_j} = -\frac{1}{\rho} \frac{\partial p}{\partial x_i} + \nu \frac{\partial^2 u_i}{\partial x_j^2} + f_i \quad (17)$$

$$\frac{\partial \rho}{\partial t} + \frac{\partial(\rho \bar{u}_j)}{\partial x_j} = 0 \quad (18)$$

$$\frac{\partial(\rho \bar{u}_i)}{\partial t} + \frac{\partial(\rho \bar{u}_i \bar{u}_j)}{\partial x_j} = -\frac{\partial \bar{p} \delta_{ij}}{\partial x_j} + 2\mu \frac{\partial \bar{S}_{ij}}{\partial x_j} + \frac{\partial \tau_{ij}^R}{\partial x_j} \quad (19)$$

As seen in Reynolds Averaged Navier-Stokes equations system, the term τ_{ij}^R is referred to as Reynolds stress tensor and is decomposed into additional unknowns that need to be solved to close the equations system. The unknowns are seen in relation (20). The Boussinesq hypothesis addresses this by assuming a linear relationship between the Reynolds stresses and the mean strain rate. The equations for the Reynolds stress tensor and from Boussinesq Hypothesis are giving in (20) and (21) respectively. Since the objective that is being addressed symbolizes an incompressible flow it implies then that the term $\frac{\bar{u}_k}{x_k} = 0$, thus, the reduction in Reynolds stresses tensor can be found in equation (22). To find the eddy viscosity term, turbulence models are then employed to solve it. Such models include the mixing length model, Spalart-Allmaras model, k- ϵ models, k- ω model, and $v^2 - f$ model. [221]

$$\tau_{ij}^R = -\rho \overline{u'_i u'_j} \quad (20)$$

$$\tau_{ij}^R = \mu_t \left[\frac{\partial \bar{u}_i}{\partial x_j} + \frac{\partial \bar{u}_j}{\partial x_i} - \frac{2}{3} \frac{\partial \bar{u}_k}{\partial x_k} \delta_{ij} \right] - \frac{2}{3} \rho k \delta_{ij} \quad (21)$$

$$\tau_{ij}^R = \mu_t \left[\frac{\partial \bar{u}_i}{\partial x_j} + \frac{\partial \bar{u}_j}{\partial x_i} \right] - \frac{2}{3} \rho k \delta_{ij} \quad (22)$$

Further, upon choosing a turbulence model, one must keep in mind how to resolve turbulence in near-wall regions. RANS models often struggle to predict the flow accurately in these regions. Thus, wall functions can be adapted to resolve the turbulence near-wall regions. Wall functions use the law of the wall theory given by the aforementioned Hungarian mathematician, Theodore von Kármán by implying the first layer at the logarithmic layer, where viscous forces aren't dominant as observed. The following implies from the equation given at (9) that the first layer can be coarser, and thus, fewer computational resources are needed. [221]

By rearranging the equation (9), the height of the first surface mesh centroid can be calculated

according to the rearranged equation (23), the wall shear stress τ in equation (24) is then calculated with complement to the skin friction coefficient C_f the depends on Reynolds number approximated by kempf-karman in equation (24)).

$$y = y^+ \frac{\mu}{\rho u_\tau} \quad (23)$$

$$\tau = C_f \frac{1}{2} \rho U_f^2 \quad (24)$$

$$C_f = 0.055 Re^{-0.182} \quad (25)$$

However, the following method wasn't used to find the first height of the the first cell from the boundary to its centroid and Aij guidelines were used since wall functions in Ansys Fluent is calculated the first layer centroid height using the expression given in (26)

$$y^* = \frac{\rho C_\mu^{0.25} K_p^{0.5} y}{\mu} \quad (26)$$

Further, to solve Reynolds stress tensor, a two-equation eddy viscosity model is used. Ansys Fluent offers k ϵ models; renormalized group (RNG), Standard and Realizable, and K ω model. Mainly, these two equations have the general form expressed in equation (27), which consists of the unsteady term, convection term, diffusion term, production term, and dissipation term, and both offer the use of wall functions. Since K ϵ models are considered to be stable and widely used in free-stream flows, it makes it a suitable turbulence model to be used to resolve the objective of the second research question. K ϵ realizable is preferred over the standard and RNG models owing to the fact that both these models fail to meet the mathematical constraints on the Reynolds stresses for consistency with the physics of turbulence. The mathematical constraint is expressed in equation (29). To address this issue professor T.H. Shih addressed this problem in the realizable model. The term ‘‘realizable’’ refers to the mode’s ability to satisfy these mathematical constraints to ensure they are consistent with the physics of turbulence. The equations for both the transport equations can be seen in equations (28 and 29). Once both of the equations are known, equation (30) is implemented to solve the turbulent viscosity term μ_t and thus, Reynolds averaged Navier-Stokes equation system can be closed. [221]

$$\frac{\partial(\rho\phi)}{\partial t} + \frac{\rho \overline{u_j' \phi}}{\partial x_j} = \frac{\partial}{\partial x_j} \left[\left(\mu + \frac{\mu_t}{\sigma} \right) \frac{\partial \phi}{\partial x_j} \right] + P_\phi + D_\phi \quad (27)$$

$$\frac{\partial(\rho k)}{\partial t} + \frac{\rho \overline{u_j} k}{\partial x_j} = \frac{\partial}{\partial x_j} \left[\left(\mu + \frac{\mu_t}{\sigma_k} \right) \frac{\partial k}{\partial x_j} \right] + P_k + D_k \quad (28)$$

$$\frac{\partial(\rho \varepsilon)}{\partial t} + \frac{\rho \overline{u_j} \varepsilon}{\partial x_j} = \frac{\partial}{\partial x_j} \left[\left(\mu + \frac{\mu_t}{\sigma_\varepsilon} \right) \frac{\partial \varepsilon}{\partial x_j} \right] + P_\varepsilon + D_\varepsilon + \rho C_1 S_\varepsilon \quad (29)$$

$$\mu_t = C_\mu \frac{k^2}{\varepsilon} \quad (30)$$

The energy equation with Boussinesq approximation that accounts for buoyancy effect in the fluid due to temperature changes is specified in equation (31). [199] Boussinesq approximation is a critical aspect to use in this study since the temperature of the occupants specified in the boundary conditions would affect the velocity field. Thus, better accuracy of chough dispersion can be achieved. [199]

$$\rho c_p \left(\frac{\partial T}{\partial t} + \vec{v} \cdot \nabla T \right) = \nabla \cdot (k \nabla T) + \Phi + S_E + \rho \beta g (T - T_{ref}) \quad (31)$$

3.3.2.3 Boundary conditions

3.3.2.3.1 Natural convection

Prior to assigning the boundary conditions at the walls of the building, the domain, the inlet, and the outlet, one must understand that choosing the correct boundary conditions is essential to obtaining accurate results that represent the correct physical realism in the calculation and to avoid divergence problems. This is necessary since compliance with the principles of fluid dynamics, and thermodynamics would affect the solution in terms of realism. To solve convection, similar studies were analyzed to see which boundary conditions were chosen to solve the physics of natural convection. It was observed that the studies aligned with Aij's guidelines, which then increased confidence. [191][192] [193] [194] [195] [187]

Boundary conditions

<i>Top boundary</i>	Symmetry
<i>Lateral boundary</i>	Symmetry
<i>Ground boundary</i>	No-slip wall
<i>Building</i>	No-slip wall
<i>Internal walls</i>	No-slip wall
<i>Occupant</i>	No-slip wall
<i>Inlet boundary</i>	Velocity inlet
<i>Outlet boundary</i>	Pressure outlet

Table 5: the boundary conditions of the domain

Further, the roughness of the walls was set to zero for smooth wall conditions. Turbulence intensity and turbulent viscosity ratio were kept to default, e.g., 5% and 10, respectively, at the outlet and the inlet. Gauge pressure was kept at zero. Gauge pressure is the pressure relative to atmospheric pressure. If it is set to zero, it ensures that the pressure variations within the flow domain are referenced to atmospheric pressure.

For the inlet velocity magnitude, the atmospheric boundary layer for the wind velocity profile shall be adequate and represent the change of velocity with respect to height. Two velocity profiles are widely used to model natural convection in CFD. These are the wind law profile and the logarithmic law profile. The choice of a suitable wind profile respects a certain height where the area of interest lies. Since the height of the building is 19.31 meters, the logarithmic wind profile is then implied. [197] To assign the velocity magnitude to respect the logarithmic wind profile, a user-defined function is created using the guidelines given in Ansys fluent tutorial. The code can be seen in figure 23. The roughness length was chosen based on the surrounding environment of the building in interest. [198]

```
#include "udf.h"

DEFINE_PROFILE(logarithmic_wind_profile, thread, position)
{
    real uref = 2.0;    // Reference wind speed
    real z0 = 0.4;     // Aerodynamic roughness length
    real href = 10.0;  // Reference height
    face_t f;
    real z, u;

    #if !RP_HOST
        // Loop over all faces in the specified thread
        begin_f_loop(f, thread)
        {
            // Get the centroid coordinates of the face
            real x[ND_ND];
            F_CENTROID(x, f, thread);

            // Extract the z-coordinate (height) from the centroid
            z = x[2];

            // Calculate velocity profile based on logarithmic wind equation
            u = uref * log(z / z0) / log(href / z0);

            // Assign the calculated velocity to the profile at the centroid of the face
            F_PROFILE(f, thread, position) = u;
        }
        end_f_loop(f, thread)
    #endif
}
```

Figure 23: UDF for the logarithmic wind profile

Type of terrain	z_0 (m)
Sand	0.0001–0.001
Sea surface	0.005
Grass	0.01–0.1
Pine forest	0.90–1.0
Suburban areas	0.20–0.40
Centers of cities	0.35–0.80

Figure 24: Roughness coefficient for different type of terrain

3.3.2.3.2 Energy setup

Since the thermal plume effect is considered in this study, the boundary conditions and with respect to gravity and energy equation choice are set as given in Table (6). It's necessary to observe that the occupant heat flux is considered to a metabolic rate that corresponds to the occupant metabolic rate of $70 \frac{W}{m^2}$. The value below in the table is given with respect to the adiabatic assumption made. Thus, radiative heat loss isn't considered and only heat loss due to convection and evaporation is considered. The occupant is assumed to have one degree higher Celsius in body temperature, which, as mentioned in chapter (2.2.1.2), corresponds to a change of 13% in metabolic rate.

Models

<i>Energy</i>	On
General	
<i>Gravity (Z)</i>	$-9.82 \frac{m}{s^2}$
Materials	
<i>Fluid (air)</i>	Density [Boussinesq] Thermal Expansion Coefficient [K ⁻¹] = 0.00338
Boundary conditions	[Thermal]
<i>Inlet boundary</i>	295.15 [K]
<i>Outlet boundary</i>	295.15 [K]
<i>Ground</i>	Heat flux $\frac{W}{m^2}$ – Adiabatic condition = 0
<i>Building</i>	Heat flux $\frac{W}{m^2}$ – Adiabatic condition = 0
<i>Interior walls</i>	Heat flux $\frac{W}{m^2}$ – Adiabatic condition = 0
<i>Occupant</i>	Heat flux $\frac{W}{m^2}$ – 47.46

Table 6: description of the thermal boundary conditions, materials, gravity and energy

Further into the methods of solution, the following scheme and spatial discretization were chosen. Second-order upwind was implemented since the first-order upwind is less accurate in approximating the convective fluxes, which then affects the result's accuracy in terms of the velocity field and energy dissipation through adjacent cells.

Methods

Pressure-velocity coupling	
<i>Scheme</i>	Simple
Spatial Discretization	
<i>Gradient</i>	Least Squares Cell Based
<i>Pressure</i>	Second Order
<i>Momentum</i>	Second Order Upwind
<i>Turbulent Kinetic Energy</i>	Second Order Upwind
<i>Turbulent Dissipation Rate</i>	Second Order Upwind
<i>Energy</i>	Second Order Upwind

Table 7: Solver methods setup

The solution controls, which represent the relaxation factors, can be changed in Ansys Fluent but were kept at default values. Furthermore, the convergence criteria is set to $*10^{-5}$ for the residuals, which describes the error in the solution in the governing equations of continuity, momentum, and energy equation.

3.3.2.3.3 Cough dispersion

The cough dispersion is modeled using the Lagrangian discrete phase within Ansys Fluent. In Ansys Fluent, each particle's trajectory is predicted using the Lagrangian reference frame, which Ansys Fluent solves by integrating the force balance equation. The equation (32) equates particle interaction with forces acting on it in the direction that the particle is bound to.

$$\frac{\partial u_p}{\partial t} = F_D(u - u_p) + \frac{g(\rho_p - \rho)}{\rho_p} + F \quad (32)$$

To model the cough dispersion, the injection type, cough diameter distribution, and velocity must be specified for the cough. Ansys Fluent offers multiple choices for specifying the diameter distribution. One can specify how and where particles are introduced to the flow field. To meet the objective of the second research question. Surface injection is specified at a surface. This surface is specified to be the mouth of the occupant which is set to be an area of

0.4 cm². [200] The initial velocity of the cough at the mouth surface was set to $11.7 \frac{m}{s}$ Which represent the average expiration air velocity of a cough.[201] Further, the cough distribution was set with respect to Rammler-Rosin diameter distribution. The data for the mean diameter, min and max diameter distribution, the spread diameter, and the mass flow rate of saliva was set with respect to experimental data modeled to fit the Rammler-Rosin distribution. [202] The duration and the amount of the cough were specified according to the same study assumptions. [202]

3.3.3 Results

The results were taken with respect to running the natural convection simulation at first to make sure that the natural convection scenario without the energy equation nor the cough dispersion converges with no issues. Only one case with wind direction coming from the east with a velocity of 2 measured at a reference height of 10 meters was simulated since this one case would be enough to give an insight if there is an issue with the geometries, mesh, or the simulation setup. Then, activating the energy equation and specifying the cough dispersion is bonded to the next models, which are specified to be 12 models in total, 6 with a wind velocity of 2 meters, and 6 with a wind velocity of 4 meters with respect to changing wind direction in 45° increments. These models were the ones of interest; therefore, the models with the energy equation and cough distribution need to be validated to make sure the results obtained respect accuracy that represent realistic scenarios. This can be made by comparing the model with experimental data through modeling velocity profiles specified at certain lines of interest.

According to the specified mesh parameters given in section x,x the natural convection scenario was simulated. The model ran to 5000 iterations with the observation that residuals converged at 1500 iterations to the data given below with almost no change or fluctuations in the solution.

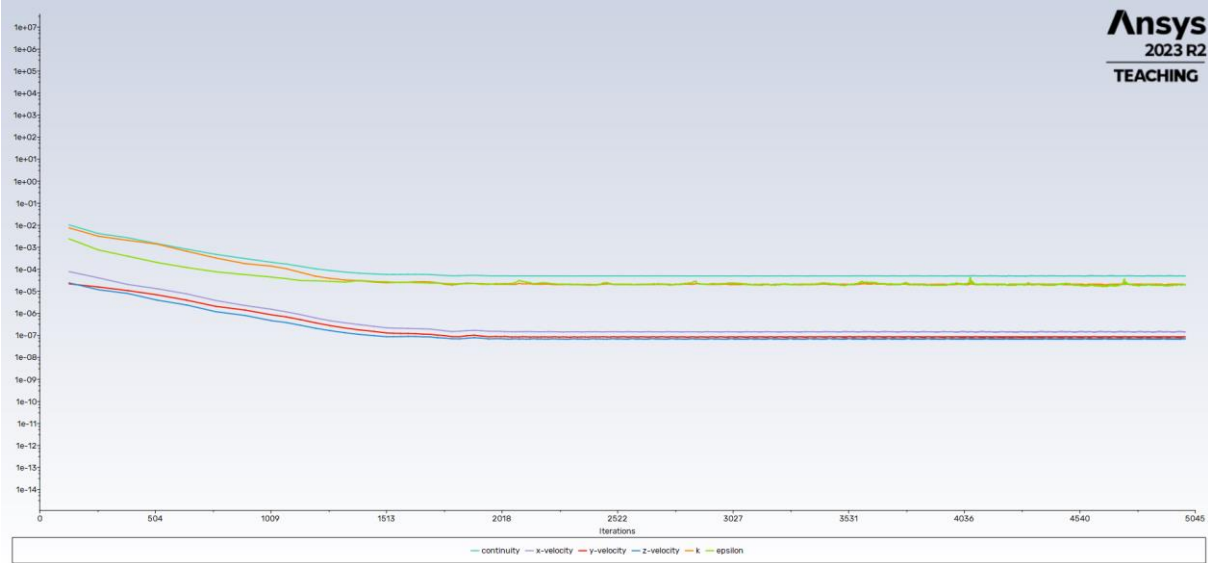


Figure 25: residuals of the natural convection solution

Residuals	Continuity	X-velocity	Y-velocity	Z-velocity	k	ϵ
<i>Solution Error</i>	$5*10^{-5}$	$1.4*10^{-7}$	$8.6*10^{-8}$	$6.9*10^{-8}$	$2*10^{-5}$	$1.9*10^{-5}$

Table 8: Residuals error values normalized

The solution converged almost by 5 folds for continuity, turbulent kinetic energy, and turbulent dissipation rate. However, the velocity field x, y, and z directions converged by 7 folds. The following solution met the criteria set, and therefore, to make sure that the solution is mesh independent, a mesh independency test was performed by changing the size of each element to one and a half in each direction, the original size in each direction. Since the objective is 3 dimensional, each element would expand by a factor of 1.5 in each direction; thus, the total size would be changed by a factor of 3.375 for each element. Table (9) gives an insight into the total elements and nodes for the coarse, medium, and fine meshes. [187]

Mesh	Total elements	Total nodes
<i>Coarse</i>	$2.3*10^6$	$0.42*10^6$
<i>Medium</i>	$5.1*10^6$	$0.9*10^6$
<i>Fine</i>	$9.77*10^6$	$1.8*10^6$

Table 9: Mesh dependence study total elements for Coarse, Medium and Fine mesh

It was observed, that all the meshes performed equally in the magnitude of error. To see if there is difference in the calculations of these 3 meshes, two dimensionless entities z/H and U/U_{ref} are plotted with a line profile from the ground of the domain to the height of the domain at certain points. These points are located at the front and behind the building, at which two are located at the leeward side away from the building and close the building. The other two points are located at the windward side of the building close and away from the building. The following ensures that mesh resolution didn't affect the solution.

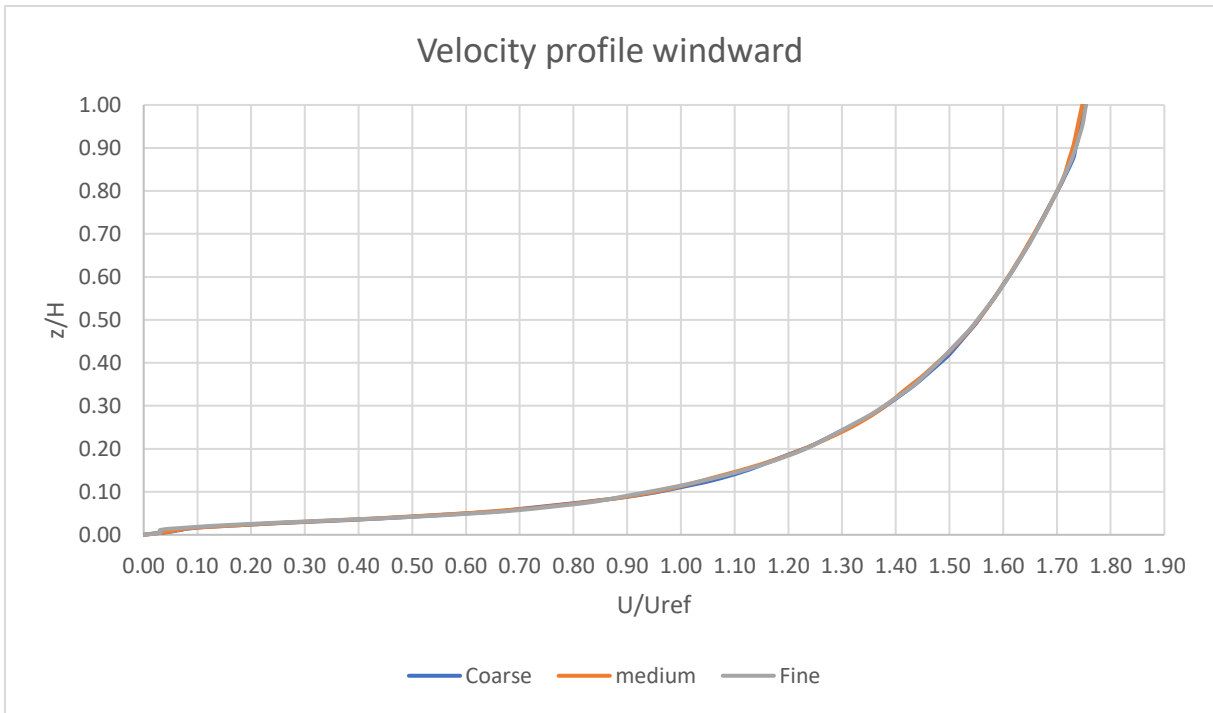


Figure 26: velocity profile at windward location

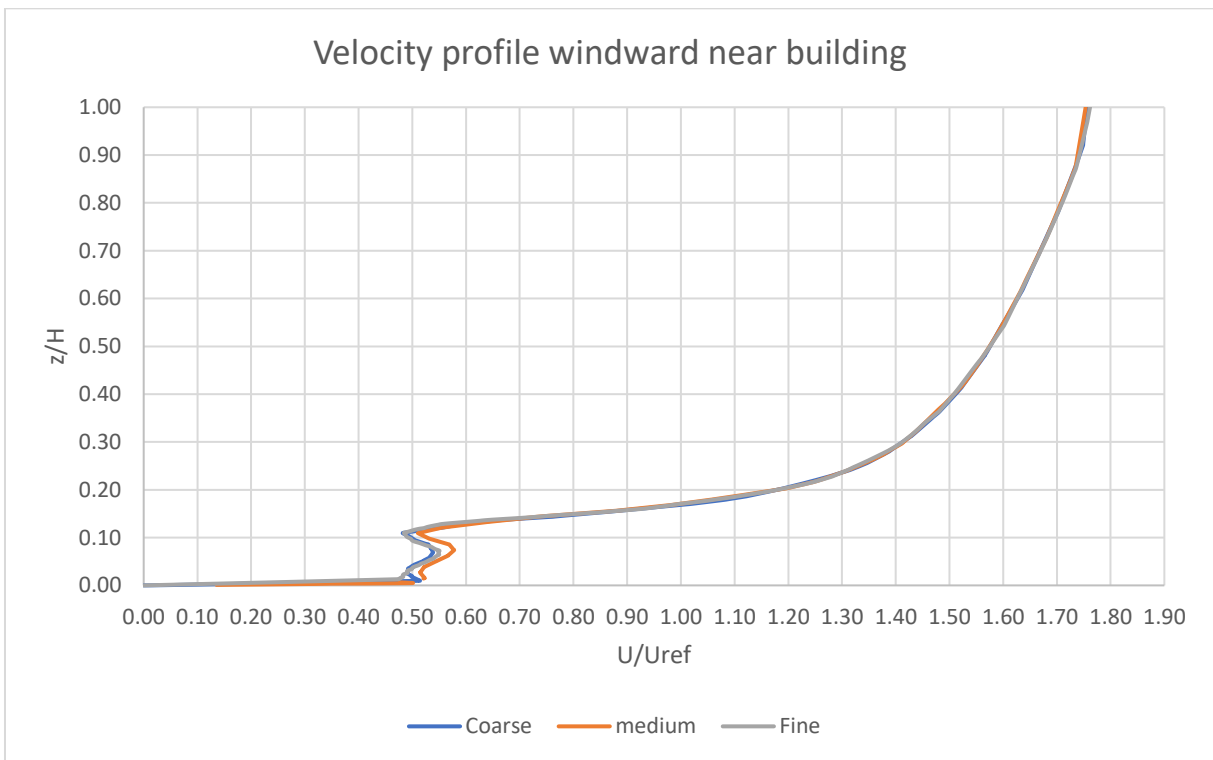


Figure 27: velocity profile at windward 1.5 meters away from the building

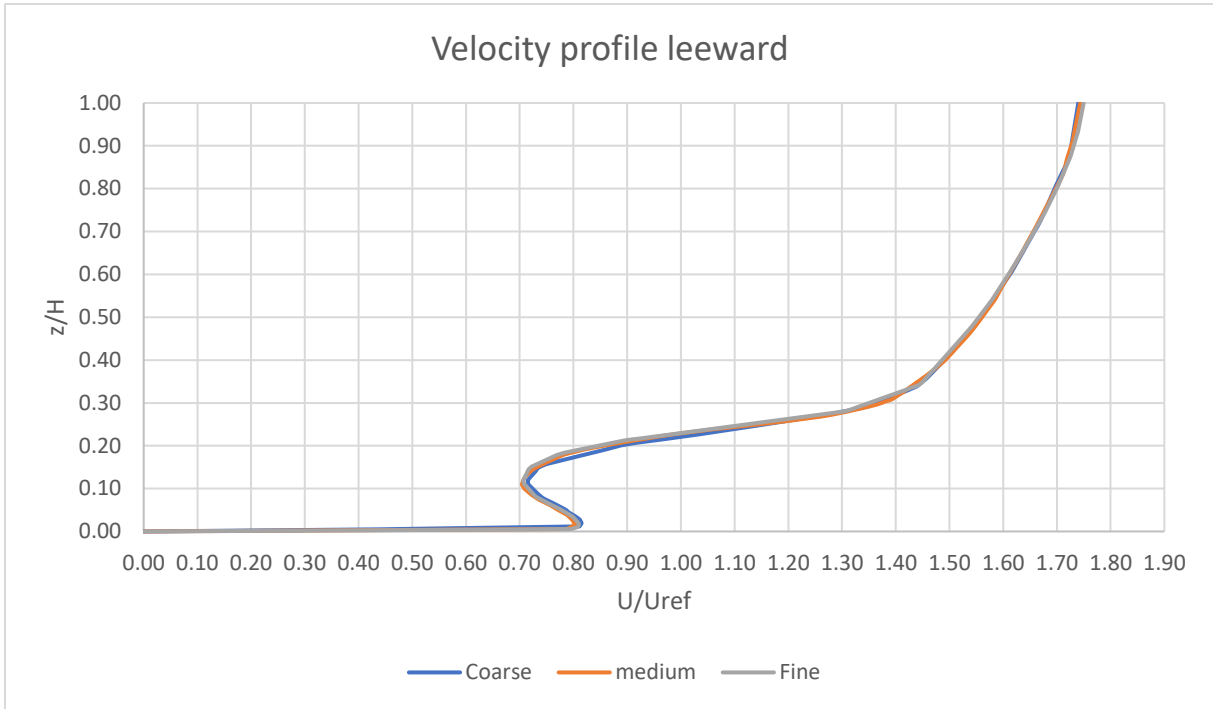


Figure 28: velocity profile at windward location

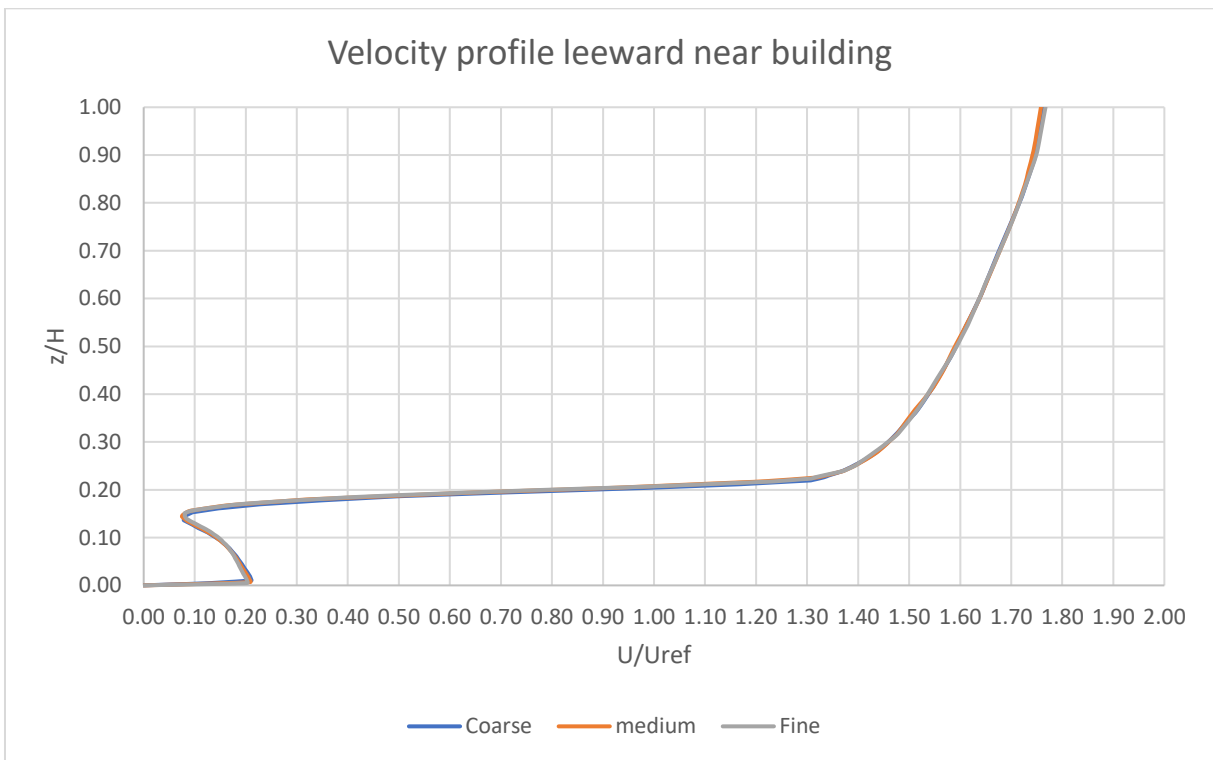


Figure 29: velocity profile at leeward 1.5 meters away from the building

As seen, the coarse mesh offers an adequate resolution for the convection problem. Thus, it was adopted for the energy equation and the particle dispersion model. Further, the energy equation was turned on, and the specification given in chapter (3.3.2.3.2) was implemented. Before activating the setup for the cough particle dispersion, a confirmation of the thermal settings had to be tested in term of convergence. With running the simulation with coarse mesh, an issue persisted with backflow on 50% of the faces on the outlet was identified on the pressure outlet. To make sure that the mesh was adequate, 2 simulations were run with the medium mesh and fine mesh. However, the issue kept on persisting.

4. Discussion

In the following thesis, two research questions were set to be answered. The first research question was necessary to identify which cases should be analyzed in terms of how the buoyancy effect, wind velocity, and direction would change the flow rate obtained at an opening. It was thus found that the flow rate does indeed get effected by altering these factors. Upon that fact, the trajectory of the cough particles injected from an occupant would be influenced by these effects where the dominating effect was explained in the chapter (3.2).

Answering the first research question gave insight into different cases where the second research question was supposed to be altered in wind direction and velocity to see how the dispersion through these windows would occur and if any of these particles would be bound to be trajected to the neighboring windows. The findings would evaluate if airborne transmission of SARS-CoV-2 was possible over distances as specified in the literature review of this master thesis. Thus, the objective of evaluating the second research question would give a clearer picture of the situation that failed to be calculated. To evaluate the cause of the issue, a systematic approach was adopted; in a sense, simulations were tested on each milestone reached to the energy equation to evaluate what was the cause of the problem. It was found through deeper evaluation that the problem persisted once density was set to Boussinesq, which models the buoyancy effect due to thermal energy. As specified in the results, the medium and the finer mesh were tested to see if the problem was occurring due to the inadequacy of the coarser mesh to obtain a solution. However, the problem kept on persisting and all the meshes couldn't achieve a converged solution.

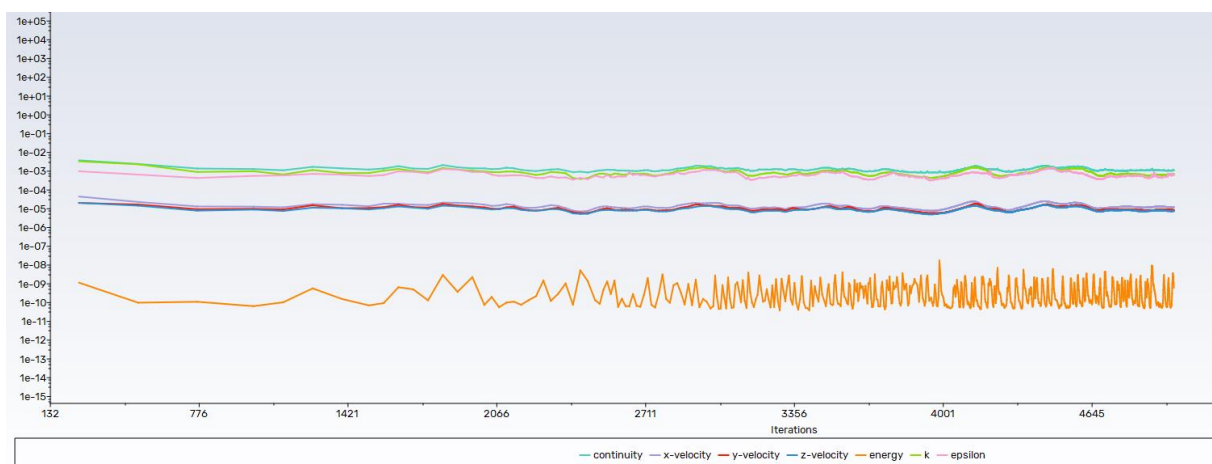


Figure 30: Residuals fluctuations and divergence - Coarse mesh

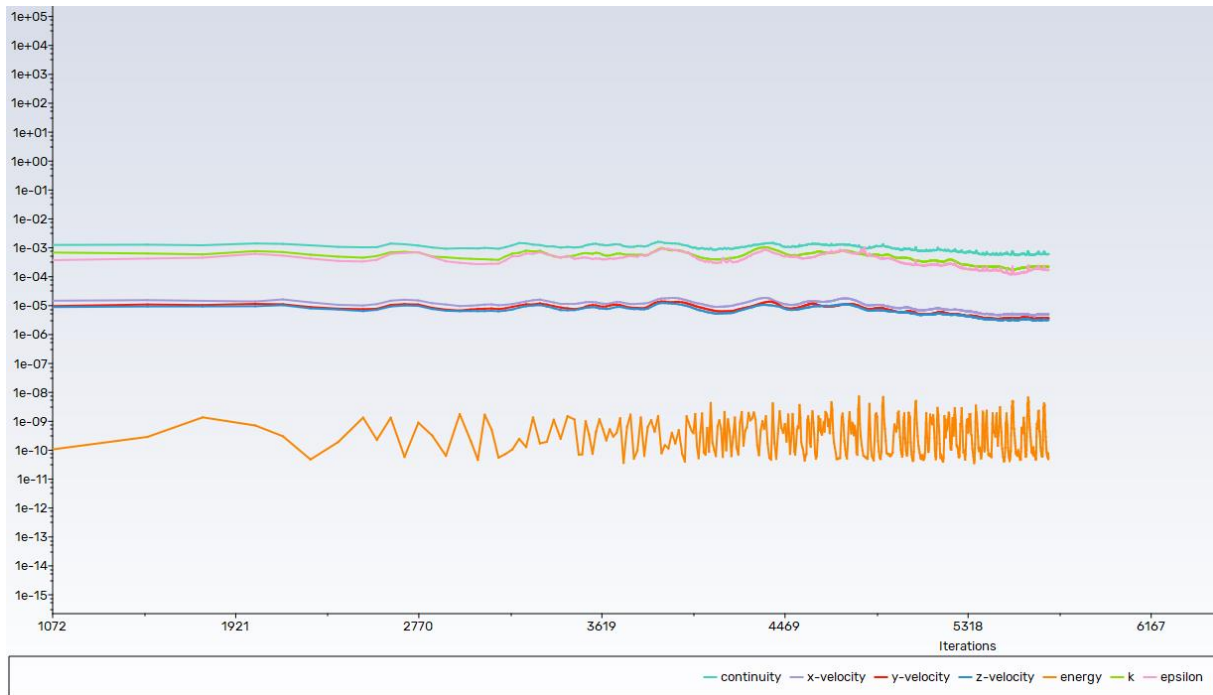


Figure 31: Residuals fluctuations and divergence - Medium mesh

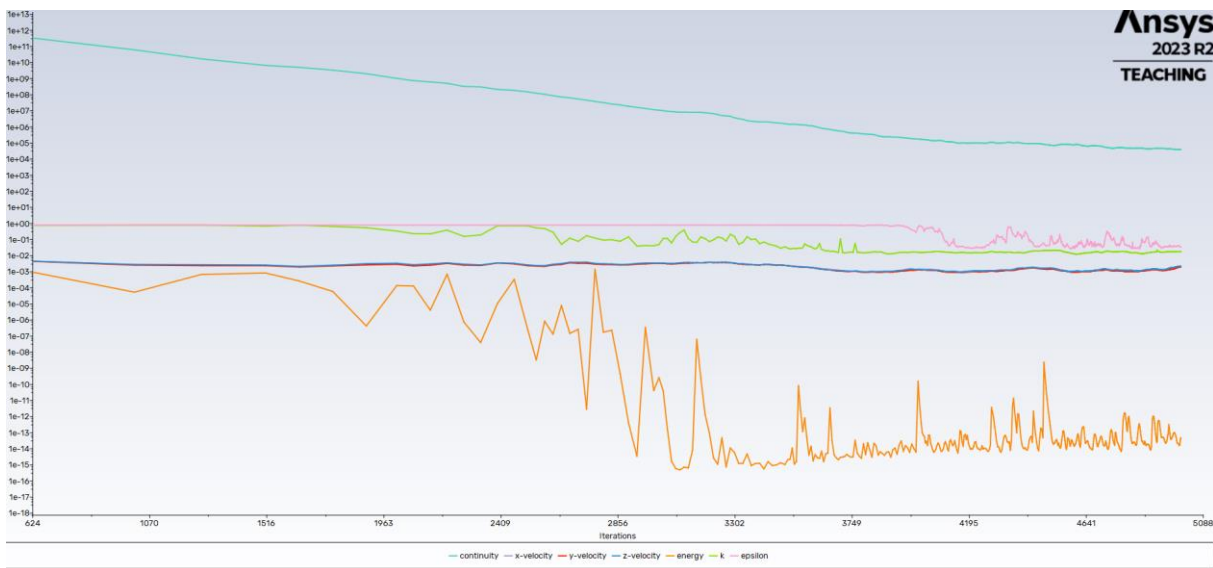


Figure 32: Residuals fluctuations and divergence - Fine mesh

G. Calzolari examined the issue persisting and concluded that the problem could be caused by the boundary conditions of the pressure outlet. A separate suggestion was made to run the simulation with ideal gas conditions; however, the problem persisted, and turbulent viscosity limitation occurred in 62530 elements with the medium mesh and 678612 elements with the fine mesh. The option was thus excluded as a solution. Upon Giovanni's suggestion, the Ansys fluent manual was examined to see if the boundary conditions of the pressure outlet

were set wrong. However, no such data was obtained leaving the second research question unresolved.

Since the energy equation seems to be the problem since the natural convection model with isothermal conditions converged, as seen in the results, similar situations have been researched to understand the cause of the problem. It was thus identified that obtaining results with energy equation is a problem occurring in studies with similar objectives and in CFD community forums [203] [204] [205] [206] [207] [208] [209] [210] [211]. Some studies suggested dropping the gauge pressure at the outlet boundary. Others suggested running the simulation of natural convection at first, then turning on the energy equation after a solution for continuity, velocity, turbulent kinetic energy, and turbulent dissipation rate is obtained. Such an approach didn't solve the objective.

One could have continued the evaluation of the dispersion of the cough particle by turning off the energy equation and assuming isothermal conditions, However, such an approach wasn't made since engaging in behaviours to improve the thermal comfort of the sick occupant considered opening the window where the dispersion would occur. Thus, implying isothermal conditions would fail to connect the objective studied with thermal discomfort. In a sense, opening a window might not occur then in the case of the sick occupant, thus, no dispersion of the virus would occur through the opened window. It is necessary to understand if a solution was obtained, it would still not give a full evaluation if a risk were imposed in terms of infection. This can be explained by the natural decay characterized by enveloped viruses due to environmental factors, as explained in the literature review, which were not evaluated in this thesis. Further, thermal effects from the building's components were set to be adiabatic, meaning no heat gain or transfer can occur between the components and the surrounding air. If no adiabatic assumption had been made, the accuracy of the model would have been better, but higher computational resources would have been needed for such a matter.

For future remarks, if the objective of a study aligns with the objective studied in this master thesis, one has to follow the initial steps for creating a model, mesh, and solve settings using the systematic approach in Figure (4), and (7). It is strongly advised to make sure that each step is controlled in terms of eliminating problems and errors. An example encountered in this thesis was the use of the digital Revit model to build the geometries of the building and the domain in ICEM. The model started at $Z = 5.05$ meters, which caused a problem later in the logarithmic wind profile used, where the Z coordinates start at $Z=0$. To resolve the problem, the Transform geometry function was in ICEM to shift the building, including the domain, to

Z=0. Thus, the model aligned with the logarithmic wind profile. One has to control the built geometries to lack any holes, which can be achieved by using the Repair geometry feature in ICEM.

5. Conclusion

Due to the persistent issue with the backflow at the pressure outlet, no conclusion can be derived on whether the dispersion of cough particles would reach the other rooms nearby.

However, through the literature review, it is noticed that virus-laden can indeed accumulate and have trajectories over long distances, making the objective studied relevant to be examined.

Through forming an understanding of particulate matter movement through fluids like air, it is understood that Buoyancy, wind velocity, and direction change the outcome of the flow rate obtained at an opening, e.g., window. The previous statement highlights that particulate matter movement through openings would be affected by the factors mentioned. If the situation is impacted and virus-laden can be deposited and extracted between indoor places through openings, a conclusion in terms of risk can be derived due to different environmental factors such as air relative humidity, temperature, and ultraviolet radiation. To summarize, an imposed risk is still in question. Analyzing the movement of particulate matter between neighboring windows can still occur. As a first step to analyze the possibility of the situation, particulate matter trajectories with respect to space and time should be analyzed. Further the natural decay of the virus-laden contained in water droplets measuring less than 5 microns should be examined through using Vero E6 cells and LLC-MK2 Cells to assess the viability of these virus-laden.

6. References

- [101] Reboucas, T (2022). *Enveloped vs. non-enveloped viruses*
[Enveloped vs. non-enveloped viruses | VIROLOGY RESEARCH SERVICES](#)
- [103] Wang, C (2021). *Airborne transmission of respiratory viruses*
[Airborne transmission of respiratory viruses | Science](#)
- [104] Nissen, K (2020). *Long-distance airborne dispersal of SARS-CoV-2*
[Long-distance airborne dispersal of SARS-CoV-2 in COVID-19 wards | Scientific Reports \(nature.com\)](#)
- [105] Silva, P (2020). *Airborne spread of infectious SARS-CoV-2: moving forward using lessons from SARS-CoV and MERS-CoV*
[Airborne spread of infectious SARS-CoV-2: Moving forward using lessons from SARS-CoV and MERS-CoV - ScienceDirect](#)
- [106] Iwamura, N (2023). *SARS-CoV-2 airborne infection probability estimated by using indoor carbon dioxide*
[SARS-CoV-2 airborne infection probability estimated by using indoor carbon dioxide | Environmental Science and Pollution Research \(springer.com\)](#)
- [107] WHO (2021). *Coronavirus disease (COVID-19): How is it transmitted?*
[Coronavirus disease \(COVID-19\): How is it transmitted? \(who.int\)](#)
- [108] SciTechDaily (2022). *COVID Gets Airborne - Expert explains how viruses travel through the air*
[COVID Gets Airborne – Expert Explains How Viruses Travel Through the Air \(scitechdaily.com\)](#)
- [109] Lewis, D (2022). *Why the WHO took two years to say COVID is airborne*
[Why the WHO took two years to say COVID is airborne \(nature.com\)](#)
- [111] Wei, J (2016). *Airborne spread of infectious agents in the indoor environment*
[Airborne spread of infectious agents in the indoor environment - ScienceDirect](#)
- [112] Prather, K (2020). *Reducing transmission of SARS-CoV-2*
[Reducing transmission of SARS-CoV-2 | Science](#)
- [113] Zhang, L (2020). *On airborne transmission and control of SARS-CoV-2*
<https://www.sciencedirect.com/science/article/pii/S0048969720326954>
- [114] Lindsley, W (2010). *Measurements of airborne influenza virus in aerosol particles from human coughs*
<https://journals.plos.org/plosone/article?id=10.1371/journal.pone.0015100>
- [116] Tang, J (2009). *The effect of environmental parameters on the survival of airborne infectious agents*
[The effect of environmental parameters on the survival of airborne infectious agents \(royalsocietypublishing.org\)](#)
- [121] Morawska, L (2020). *It is time to address airborne transmission of coronavirus disease 2019* [It Is Time to Address Airborne Transmission of Coronavirus Disease 2019 \(COVID-19\) | Clinical Infectious Diseases | Oxford Academic \(oup.com\)](#)
- [122] REHVA (n.d.). *REHVA*
[About us \(rehva.eu\)](#)
- [123] Cao, J (2020). *Airborne Transmission of SARS-CoV-2: The world should face the reality*
[Airborne transmission of SARS-CoV-2: The world should face the reality - ScienceDirect](#)
- [124] Li, Y (2016.). *Airborne spread of infectious agents in the indoor environment*
[Airborne spread of infectious agents in the indoor environment - American Journal of Infection Control \(ajicjournal.org\)](#)
- [125] Miller, S (2016.). *Transmission of SARS-CoV-2 by inhalation of respiratory aerosol in the Skagit Valley Chorale superspreading event*
[Transmission of SARS-CoV-2 by inhalation of respiratory aerosol in the Skagit Valley Chorale superspreading event - PubMed \(nih.gov\)](#)
- [126] Qian, H (2021). *Probable airborne transmission of SARS-CoV-2 in a poorly ventilated restaurant*
[Probable airborne transmission of SARS-CoV-2 in a poorly ventilated restaurant - ScienceDirect](#)
- [130] Mohamadi, F (2022). *A review on applications of CFD modeling in COVID-19 pandemic*
[A Review on Applications of CFD Modeling in COVID-19 Pandemic - PMC \(nih.gov\)](#)
- [132] Environment europe (n.d.) *EU air quality standards*
[EU air quality standards - European Commission \(europa.eu\)](#)
- [133] IQair (n.d.) *Live most polluted major city ranking*
[World Air Quality Index \(AQI\) Ranking | IQAir](#)
- [135] Saadat, S (2020) *Environmental perspective of COVID-19*
[Environmental perspective of COVID-19 - ScienceDirect](#)
- [136] Sharma, S (2020) *Effect of restricted emissions during COVID-19 on air quality India*

- [Effect of restricted emissions during COVID-19 on air quality in India - ScienceDirect](#)
- [137] Helm, D (2020) *The environmental impacts of the coronavirus*
[The Environmental Impacts of the Coronavirus | Environmental and Resource Economics \(springer.com\)](#)
- [139] Park, J (2020) *Effect of types of ventilation system on indoor particle concentrations in residential buildings*
[Effects of types of ventilation system on indoor particle concentrations in residential buildings - Park - 2014 - Indoor Air - Wiley Online Library](#)
- [140] Lv, Y (2017) *The correlation between indoor and outdoor particulate matter of different building types in Daqing, China*
[The Correlation between Indoor and Outdoor Particulate Matter of Different Building Types in Daqing, China - ScienceDirect](#)
- [142] Koponen, I (2001) *Indoor air measurement campaign in Helsinki, Finland 1999*
[Indoor air measurement campaign in Helsinki, Finland 1999 – the effect of outdoor air pollution on indoor air - ScienceDirect](#)
- [143] Quang, T (2013) *Influence of ventilation on filtration on indoor particle concentration in urban office buildings*
[Influence of ventilation and filtration on indoor particle concentrations in urban office buildings - ScienceDirect](#)
- [144] Yu, B.F (2009) *Review of research on air-conditioning systems and indoor air quality control for human health*
[Review of research on air-conditioning systems and indoor air quality control for human health - ScienceDirect](#)
- [145] Orch, Z (2014) *Predictions and determinants of size-resolved particle infiltration factors in single-family homes in the U.S.*
[Predictions and determinants of size-resolved particle infiltration factors in single-family homes in the U.S. - ScienceDirect](#)
- [146] Nazaroff, W (2001) *Modeling pollutant penetration across building envelopes*
[Modeling pollutant penetration across building envelopes - ScienceDirect](#)
- [147] Su, W (2023) *Maintaining an acceptable indoor air quality of spaces by intentional natural ventilation or intermittent mechanical ventilation with minimum energy use*
[Maintaining an acceptable indoor air quality of spaces by intentional natural ventilation or intermittent mechanical ventilation with minimum energy use - ScienceDirect](#)
- [148] IECPR (n.d.) *IAQ Facts* [IEC / Indoor Environmental Consultants » IAQ Facts \(iec-pr.net\)](#)
- [149] Sustainable facilities (n.d.) *Indoor Environmental Quality (IEQ)*
[Indoor Environmental Quality \(IEQ\) - GSA Sustainable Facilities Tool \(sftool.gov\)](#)
- [154] UnuEdu (n.d.) *Effects of infection on energy status*
[A better way to predict comfort: the new ASHRAE standard 55-2004 \(escholarship.org\)](#)
- [155] ASHRAE Standard 55-2017 (2017) *Thermal environmental conditions for human occupancy* [55_2017_d_20200731.pdf \(ashrae.org\)](#)
- [156] same as 155] [ASHRAE - iWrapper](#)
- [157] Wilde, J (2023) *Indoor Thermal standards*
[Indoor Thermal Standards: ASHRAE 55 vs. ISO 7730 | SimScale](#)
- [158] Olesen, B (2023) *Revision of EN 15251: Indoor Environmental Criteria*
[revision-of-en-15251_rj1204.pdf \(rehva.eu\)](#)
- [160] Saint gobain (2019) *How to design for visual comfort using natural light*
[How to design for visual comfort using natural light | Saint-Gobain](#)
- [161] Thesoundproofofwindows (2024) *Acoustic Glazing*
[Noise Reduction Glass | Soundproof Windows - Soundproof Windows \(thesoundproofwindows.co.uk\)](#)
- [162] Ganesh, G (2021) *Investigation of indoor environment quality and factors affecting human comfort*
[Investigation of indoor environment quality and factors affecting human comfort: A critical review - ScienceDirect](#)
- [163] same as 161] [Noise Reduction Glass | Soundproof Windows - Soundproof Windows \(thesoundproofwindows.co.uk\)](#)
- [164] Fanger, P.O (2007) *Can colour and noise influence Man's thermal comfort*
[Can Colour and Noise Influence Man's Thermal Comfort?: Ergonomics: Vol 20, No 1 \(tandfonline.com\)](#)
- [165] Frontczak, M (2011) *Literature survey on how different factors influence human comfort in indoor environments*
[Literature survey on how different factors influence human comfort in indoor environments - ScienceDirect](#)
- [166] Acoust, J (2008) *Subjective and objective assessment of acoustical and overall environmental quality in secondary school classrooms*
[Subjective and objective assessment of acoustical and overall environmental quality in secondary school classrooms | The Journal of the Acoustical Society of America | AIP Publishing](#)
- [168] Humphreys, M (2007) *Quantifying occupant comfort: are combined indices of the indoor environment practicable*
[Full article: Quantifying occupant comfort: are combined indices of the indoor environment practicable? \(tandfonline.com\)](#)
- [169] Lai, A.C.K (2009) *An evaluation model for indoor environmental quality acceptance in residential buildings*
[An evaluation model for indoor environmental quality \(IEQ\) acceptance in residential buildings - ScienceDirect](#)

- [170] Lai, J (2007) *Perceived importance of the quality of the indoor environment in commercial buildings*
[Perceived Importance of the Quality of the Indoor Environment in Commercial Buildings - Joseph H. K. Lai, Francis W. H. Yik, 2007 \(sagepub.com\)](#)
- [171] Yik, F (2009) *Perception of importance and performance of the indoor environmental quality of high-rise residential buildings*
[Perception of importance and performance of the indoor environmental quality of high-rise residential buildings - ScienceDirect](#)
- [172] Wong, L.T (2008) *A multivariate-logistic model for acceptance of indoor environmental quality in offices*
[A multivariate-logistic model for acceptance of indoor environmental quality \(IEQ\) in offices - ScienceDirect](#)
- [173] Rindel, J (1993) *A comparative study of discomfort caused by indoor air pollution, thermal load and noise*
[A Comparative Study Of Discomfort Caused By Indoor Air Pollution, Thermal Load And Noise - Clausen - 1993 - Indoor Air - Wiley Online Library](#)
- [175] Ekici, C (2013) *A review of thermal comfort method of using Fanger's PMV equation*
[\(PDF\) A review of thermal comfort and method of using Fanger's PMV equation \(researchgate.net\)](#)
- [176] CuErgo (n.d.) *Thermal environment*
[Thermal Comfort Lecture 2 \(cornell.edu\)](#)
- [177] OECD (2004) *OECD work on sustainable buildings*
[OECD Work on Sustainable Buildings - OECD](#)
- [178] Zhang, M (2024) *Natural ventilation for cooling energy saving: typical case of public building design optimization in Guangzhou, China*
[Applied Sciences | Free Full-Text | Natural Ventilation for Cooling Energy Saving: Typical Case of Public Building Design Optimization in Guangzhou, China \(mdpi.com\)](#)
- [179] Ugreen(u.d.) *The benefits of natural ventilation: improved air quality, cost savings, and sustainability*
[Natural Ventilation and Energy Efficiency: Reducing Costs \(ugreen.io\)](#)
- [180] WHOa (u.d.) *Coronavirus disease*
[Coronavirus \(who.int\)](#)
- [181] Penn medicine (u.d.) *Fever*
[Fever - Symptoms and Causes \(penncornell.edu\)](#)
- [182] KTH (u.d.) *KTH U-group rooms*
[KTH | Sök](#)
- [186] Xu, G (2021) *Airborne dispersion of droplets during coughing*
[Airborne dispersion of droplets during coughing: a physical model of viral transmission | Scientific Reports \(nature.com\)](#)
- [187] Tominaga, Y (2008) *AIJ guidelines for practical applications of CFD to pedestrian wind environment around buildings*
[AIJ guidelines for practical applications of CFD to pedestrian wind environment around buildings - ScienceDirect](#)
- [188] Franke, J (2004) *Recommendations on the use of CFD in wind engineering*
[\(PDF\) Recommendations on the use of CFD in wind engineering \(researchgate.net\)](#)
- [190] CFDexperts (2021) *CFD experts, simulate the future*
[Ansys ICEM CFD Users Manual.pdf \(cfdexperts.net\)](#)
- [191] Yoshie, R (2007) *Cooperative project for CFD prediction of Pedestrian wind environment in the architectural institute of Japan*
<https://www.sciencedirect.com/science/article/pii/S0167610507000645#bib4>
- [192] Stathopoulos, T (1996) *Computer simulation of wind environmental conditions around buildings*
[Computer simulation of wind environmental conditions around buildings - ScienceDirect](#)
- [193] Stasi, R (2024) *Natural ventilation effectiveness in low-income housing to challenge energy poverty*
<https://www.sciencedirect.com/science/article/pii/S0378778823010666#b0395>
- [194] Ziarani, N (2023) *The role of near-façade flow in wind-dominant single-sided natural ventilation for an isolated three-storey building*
[The role of near-façade flow in wind-dominant single-sided natural ventilation for an isolated three-storey building: An LES study - ScienceDirect](#)
- [195] HE, R (2017) *Full numerical simulation on the wind driven natural ventilation across traditional songqing stadium*
[Full Numerical simulation on the Wind Driven Natural Ventilation across Traditional Songqing Stadium Established Since 1936 in Wuhan University - ScienceDirect](#)[196]
- [197] Malinowski, S (2017) *Planetary boundary layer and atmospheric turbulence*
[wyklad07_ang.pdf \(fuw.edu.pl\)](#)
- [198] Chiba, N (2011) *Type of terrain*

[VALUES OF ROUGHNESS LENGTH \$z_0\$ | Download Table \(researchgate.net\)](#)

[199] Ansys AFS (n.d.) *Natural convection and buoyancy-driven flows*

[ANSYS FLUENT 12.0 User's Guide - 13.2.4 Natural Convection and Buoyancy-Driven Flows \(enea.it\)](#)

[200] Oh, W (2022) *Numerical modeling of cough airflow*

[Numerical modeling of cough airflow: Establishment of spatial-temporal experimental dataset and CFD simulation method - ScienceDirect](#)

[201] Kwon, S.B (2012) *Study on the initial velocity distribution of exhaled air from coughing and speaking*

[Study on the initial velocity distribution of exhaled air from coughing and speaking - PMC \(nih.gov\)](#)

[203] Ansys forum (2022) *Continuity not converging in steady state*

[Continuity not Converging in Steady State \(Energy Equation OFF\) \(ansys.com\)](#)

[204] Reddit community (2017) *Problems with solving energy equation*

[Problems with solving energy equation \(Rapid Divergence and no coupling thermal?\) : r/CFD \(reddit.com\)](#)

[206] Researchgate (2016) *Fatal error*

[Can anyone see this problem in openfoam?can anyone solve it? | ResearchGate](#)

[210] Thompson, M (2017) *Energy error*

[Energy Error - an overview | ScienceDirect Topics](#)

[212] Idealsimulations (n.d.) *What is turbulent flow?*

[Turbulence models in CFD - RANS, DES, LES and DNS \(idealsimulations.com\)](#)

[214] Homepages (n.d.) *Viscosity and shear stresses*

[Notes_Viscosity.pdf \(ucl.ac.uk\)](#)

[216] Asp, M (2022) *Wind roses for analysis of local wind conditions*

[Wind roses for analysis of local wind conditions | SMHI](#)

[217] Malmsten, S(n.d.) *Wind rose*

[windrose.pdf \(smhi.se\)](#)

[218] Sultan, S (2010) *Wind turbulence*

[Wind Turbulence - an overview | ScienceDirect Topics](#)

[219] Nebenfuhr, B (2015) *Turbulence-resolving simulations for engineering applications* [bastian_phd.pdf \(chalmers.se\)](#)

[220] Wooding, S (2024) *Y+calculator*

[Y+ Calculator \(omnicalculator.com\)](#)

[222] CFDblogs (2024) *Wall functions*

[Wall functions | Introduction to CFD \(upv.es\)](#)

[223] Larsen, T (2008) *Single-sided natural ventilation driven by wind pressure and temperature difference*

[Single-sided natural ventilation driven by wind pressure and temperature difference - ScienceDirect](#)

[224] Warren, P.R (1985) *Single-sided ventilation through open window*

[Single-sided ventilation through open window | CiNii Research](#)

[225] Warren, P.R (1997) *Ventilation Through openings on one wall only*

[airbase_00026.pdf \(aivc.org\)](#)

A. Appendices

A.1 Appendix

Wells Riley equation

$$P_I = \frac{C}{S} = 1 - e^{-\frac{Iqpt}{Q}} \quad (33)$$

P_I : probability of infection

C : number of infection cases

S : number of susceptibles

I : number of infectors

q : quanta generation rate

p : pulmonary ventilation rate

t : exposure time interval

Q : room ventilation rate

A.2 Appendix

Predicted mean vote equation

$$PMV = \frac{(M-W)+(R-C)+(C-K)+(E-H)}{0.303 * e^{(-0.036 * M + 0.028 * W + 0.42 * R + 0.72 * C + 0.048 * E - 0.0043 * M * E + 0.0021 * M * E^2 - 0.0001 * M * E^3 + 0.158 * H)}} \quad (34)$$

M : metabolic rate [met]

W : external work [met]

R : radiant heat exchance [W/m^2]

C : Convective heat exchange [W/m^2]

K : thermal conductance of clothing [$W/m^2 * K$]

E : water vapor permeability of clothing [$Pa/m^2 * s$]

H : relative humidity [%]

Predicted mean vote equation

$$PPD = 100 * (1 - \frac{1}{1 + e^{(16.6 * (PMV - 0.5))}})$$
 (35)

A.3 Appendix

Apple lidar sensor offered in the model iPhone 12 Pro can be used in many applications, such as enhancing the camera focusing ability. However, Apple featured in their phones since the iPhone 12 models a measurement function using the Lidar sensor. The accuracy had to be evaluated of the scanner since some manual measurements were made of areas that couldn't be reached in this thesis. It was found to offer an accuracy of 4.89 mm in error from real measurement. Thus, Making the measurement method valid for use. [184]

A.4 Appendix

$$y = y_1 + \frac{y_2 - y_1}{x_2 - x_1} * (x - x_1)$$
 (36)